

## Interleaving Continuous Conduction Mode PFC Controller

### FEATURES

- Interleaved Average Current-Mode PWM Control with Inherent Current Matching
- Advanced Current Synthesizer Current Sensing for Superior Efficiency
- Highly-Linear Multiplier Output with Internal Quantized Voltage Feed-Forward Correction for Near-Unity PF
- Programmable Frequency (10 kHz to 300 kHz)
- Programmable Maximum Duty-Cycle Clamp
- Programmable Frequency Dithering Rate and Magnitude for Enhanced EMI Reduction
  - Magnitude: 3 kHz to 30 kHz
  - Rate: Up to 30 kHz
- External Clock Synchronization Capability
- Enhanced Load and Line Transient Response through Voltage Amplifier Output Slew-Rate Correction
- Programmable Peak Current Limiting
- Bias-Supply UVLO, Over-Voltage Protection, Open-Loop Detection, and PFC-Enable Monitoring
- External PFC-Disable Interface
- Open-Circuit Protection on VSENSE and VINAC pins
- Programmable Soft Start
- 20-Lead TSSOP Package

### APPLICATIONS

- High-Efficiency Server and Desktop Power Supplies
- Telecom Rectifiers

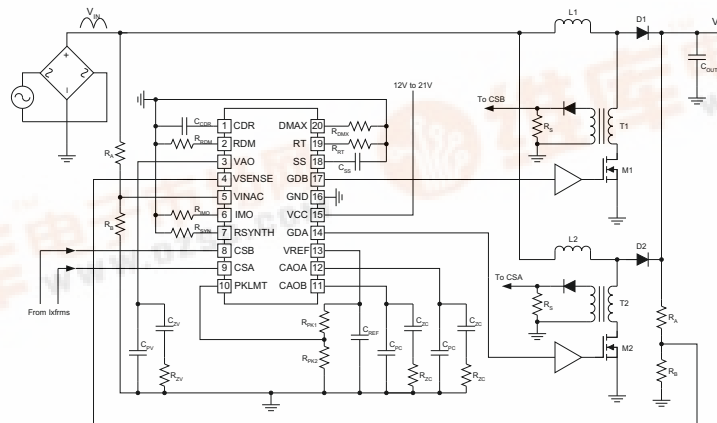
### DESCRIPTION

The UCC28070 is an advanced power factor correction device that integrates two pulse-width modulators (PWMs) operating 180° out of phase. This interleaved PWM operation generates substantial reduction in the input and output ripple currents, and the conducted-EMI filtering becomes easier and less expensive. A significantly improved multiplier design provides a shared current reference to two independent current amplifiers that ensures matched average current mode control in both PWM outputs while maintaining a stable, low-distortion sinusoidal input line current.

The UCC28070 contains multiple innovations including current synthesis and quantized voltage feed-forward to promote performance enhancements in PF, efficiency, THD, and transient response. Features including frequency dithering, clock synchronization, and slew rate enhancement further expand the potential performance enhancements.

The UCC28070 also contains a variety of protection features including output over-voltage detection, programmable peak-current limit, under-voltage lockout, and open-loop protection.

Simplified Application Diagram



Please be aware that an important notice concerning availability, standard warranty, and use in critical applications of Texas Instruments semiconductor products and disclaimers thereto appears at the end of this data sheet.

**ORDERING INFORMATION**

| PART NUMBER | PACKAGE                    | PACKING                |
|-------------|----------------------------|------------------------|
| UCC28070PW  | Plastic, 20-Pin TSSOP (PW) | 70-Pc. Tube            |
| UCC28070PWR | Plastic, 20-Pin TSSOP (PW) | 2000-Pc. Tape and Reel |

**ABSOLUTE MAXIMUM RATINGS**<sup>(1)(2)(3)(4)</sup>

over operating free-air temperature range (unless otherwise noted)

| PARAMETER  | LIMIT           | UNIT |
|--|-----------------|------|
| Supply voltage: VCC  | 22              | V    |
| Supply current: I <sub>VCC</sub>   | 20              | mA   |
| Voltage: GDA, GDB  | -0.5 to VCC+0.3 | V    |
| Gate drive current – continuous: GDA, GDB  | +/- 0.25        | A    |
| Gate drive current – pulsed: GDA, GDB  | +/- 0.75        |      |
| Voltage: DMAX, RDM, RT, CDR, VINAC, VSENSE, SS, VAO, IMO, CSA, CSB, CAO, CAOB, PKLMT, VREF | -0.5 to +7      | V    |
| Current: RT, DMAX, RDM, RSYNTH   | -0.5            | mA   |
| Current: VREF, VAO, CAO, CAOB, IMO   | 10              |      |
| Operating junction temperature, T <sub>J</sub>   | -40 to +125     | °C   |
| Storage temperature, T <sub>STG</sub>  | -65 to +150     |      |
| Lead temperature (10 seconds)  | 260             |      |

- (1) These are stress limits. Stress beyond these limits may cause permanent damage to the device. Functional operation of the device at these or any conditions beyond those indicated under RECOMMENDED OPERATING CONDITIONS is not implied. Exposure to absolute maximum rated conditions for extended periods of time may affect device reliability.
- (2) All voltages are with respect to GND.
- (3) All currents are positive into the terminal, negative out of the terminal.
- (4) In normal use, terminals GDA and GDB are connected to an external gate driver and are internally limited in output current.

**ELECTROSTATIC DISCHARGE (ESD) PROTECTION**

|                            | RATING | UNIT |
|----------------------------|--------|------|
| Human Body Model (HBM)     | 2,000  | V    |
| Charged Device Model (CDM) | 500    |      |

**DISSIPATION RATINGS**

| PACKAGE      | THERMAL IMPEDANCE<br>JUNCTION-TO-AMBIENT      | T <sub>A</sub> = 25°C POWER<br>RATING | T <sub>A</sub> = 85°C POWER RATING |
|--------------|---|---------------------------------------|------------------------------------|
| 20-Pin TSSOP | 125 °C/Watt <sup>(1)</sup> and <sup>(2)</sup> | 800 mW <sup>(1)</sup>                 | 320 mW <sup>(1)</sup>              |

- (1) Thermal resistance is a strong function of board construction and layout. Air flow reduces thermal resistance. This number is only a general guide.
- (2) Thermal resistance calculated with a low-K methodology.

**RECOMMENDED OPERATING CONDITIONS**

over operating free-air temperature range (unless otherwise noted)

| PARAMETER                                       | MIN                     | MAX | UNIT |
|---|-------------------------|-----|------|
| VCC Input Voltage (from a low-impedance source) | V <sub>UVLO</sub> + 1 V | 21  | V    |
| VREF Load Current                               |                         | 2   | mA   |
| VINAC Input Voltage Range                       | 0                       | 3   | V    |
| IMO Voltage Range                               | 0                       | 3.3 |      |
| PKLMT, CSA, & CSB Voltage Range                 | 0                       | 3.6 |      |
| RSYNTH Resistance (R <sub>SYN</sub> )           | 15                      | 750 | kΩ   |
| RDM Resistance (R <sub>RDM</sub> )              | 30                      | 330 |      |

## ELECTRICAL CHARACTERISTICS

over operating free-air temperature range  $-40^{\circ}\text{C} < T_A < 125^{\circ}\text{C}$ ,  $T_J = T_A$ ,  $V_{CC} = 12\text{ V}$ ,  $GND = 0\text{ V}$ ,  $R_{RT} = 75\text{ k}\Omega$ ,  $R_{DMX} = 68.1\text{ k}\Omega$ ,  $R_{RDM} = R_{SYN} = 100\text{ k}\Omega$ ,  $C_{CDR} = 2.2\text{ nF}$ ,  $C_{SS} = C_{VREF} = 0.1\text{ }\mu\text{F}$ ,  $C_{VCC} = 1\text{ }\mu\text{F}$ , (unless otherwise noted)

| SYMBOL                                    | PARAMETER   | TEST CONDITIONS  | MIN  | TYP  | MAX  | UNITS         |
|---|---|--|------|------|------|---------------|
| <b>Bias Supply</b>                        |   |  |      |      |      |               |
| $V_{CC\text{SHUNT}}$                      | VCC shunt voltage <sup>(1)</sup>                            | $I_{VCC} = 10\text{ mA}$   | 23   | 25   | 27   | V             |
|   | VCC current, disabled                                       | $V_{SENSE} = 0\text{ V}$   |      | 7    |      | mA            |
|   | VCC current, enabled  | $V_{SENSE} = 3\text{ V}$ (switching)   |      | 9    | 12   |               |
|   | VCC current, UVLO   | $V_{CC} = 7\text{ V}$  |      |      | 200  | $\mu\text{A}$ |
|   |   | $V_{CC} = 9\text{ V}$  |      | 4    | 6    | mA            |
| $V_{UVLO}$                                | UVLO turn-on threshold                                      | Measured at VCC (rising)   | 9.8  | 10.2 | 10.6 | V             |
|   | UVLO hysteresis   | Measured at VCC (falling)  |      | 1    |      |               |
|   | VREF enable threshold                                       | Measured at VCC (rising)   | 7.5  | 8    | 8.5  |               |
| <b>Linear Regulator</b>                   |   |  |      |      |      |               |
|   | VREF voltage, no load                                       | $I_{VREF} = 0\text{ mA}$   | 5.82 | 6    | 6.18 | V             |
|   | VREF load rejection   | Measured as the change in VREF, ( $I_{VREF} = 0\text{ mA}$ and $-2\text{ mA}$ )                                    | -12  |      | 12   | mV            |
|   | VREF line rejection   | Measured as the change in VREF, ( $V_{CC} = 11\text{ V}$ and $20\text{ V}$ , $I_{VREF} = 0\text{ }\mu\text{A}$ )   | -12  |      | 12   |               |
| <b>PFC Enable</b>                         |   |  |      |      |      |               |
| $V_{EN}$                                  | Enable threshold  | Measured at VSENSE (rising)  | 0.65 | 0.75 | 0.85 | V             |
|   | Enable hysteresis   |  |      | 0.15 |      |               |
| <b>External PFC Disable</b>               |   |  |      |      |      |               |
|   | Disable threshold   | Measured at SS (falling)   | 0.5  | 0.6  |      | V             |
|   | Hysteresis  | $V_{SENSE} > 0.85\text{ V}$  |      | 0.15 |      |               |
| <b>Oscillator</b>                         |   |  |      |      |      |               |
|   | Output phase shift  | Measured between GDA and GDB   | 179  | 180  | 181  | Degree        |
| $V_{D\text{MAX}}, V_{RT}$ , and $V_{RDM}$ | Timing regulation voltages                                  | Measured at DMAX, RT, & RDM  | 2.91 | 3    | 3.09 | V             |
| $f_{\text{PWM}}$                          | PWM switching frequency                                     | $R_{RT} = 750\text{ k}\Omega$ , $R_{DMX} = 681\text{ k}\Omega$ , $V_{RDM} = 0\text{ V}$ , $V_{CDR} = 6\text{ V}$   | 9.5  | 10   | 10.5 | kHz           |
|   |   | $R_{RT} = 75\text{ k}\Omega$ , $R_{DMX} = 68.1\text{ k}\Omega$ , $V_{RDM} = 0\text{ V}$ , $V_{CDR} = 6\text{ V}$   | 95   | 100  | 105  |               |
|   |   | $R_{RT} = 24.9\text{ k}\Omega$ , $R_{DMX} = 22.6\text{ k}\Omega$ , $V_{RDM} = 0\text{ V}$ , $V_{CDR} = 6\text{ V}$ | 270  | 290  | 330  |               |
| $D_{\text{MAX}}$                          | Duty-cycle clamp  | $R_{RT} = 75\text{ k}\Omega$ , $R_{DMX} = 68.1\text{ k}\Omega$ , $V_{RDM} = 0\text{ V}$ , $V_{CDR} = 6\text{ V}$   | 92%  | 95%  | 98%  |               |
|   | Minimum programmable off-time                               | $R_{RT} = 24.9\text{ k}\Omega$ , $R_{DMX} = 22.6\text{ k}\Omega$ , $V_{RDM} = 0\text{ V}$ , $V_{CDR} = 6\text{ V}$ | 50   | 150  | 250  | ns            |
| $f_{\text{DM}}$                           | Frequency dithering magnitude change in $f_{\text{PWM}}$    | $R_{RDM} = 316\text{ k}\Omega$ , $R_{RT} = 75\text{ k}\Omega$  | 2    | 3    | 4    | kHz           |
|   |   | $R_{RDM} = 31.6\text{ k}\Omega$ , $R_{RT} = 24.9\text{ k}\Omega$   | 24   | 30   | 36   |               |
| $f_{\text{DR}}$                           | Frequency dithering rate rate of change in $f_{\text{PWM}}$ | $C_{CDR} = 2.2\text{ nF}$ , $R_{RDM} = 100\text{ k}\Omega$   |      | 3    |      |               |
|   |   | $C_{CDR} = 0.3\text{ nF}$ , $R_{RDM} = 100\text{ k}\Omega$   |      | 20   |      |               |
| $I_{\text{CDR}}$                          | Dither rate current   | Measure at CDR (sink and source)   |      | 10   |      | $\mu\text{A}$ |
|   | Dither disable threshold                                    | Measured at $C_{CDR}$ (rising)   |      | 5    | 5.25 | V             |

- (1) Excessive VCC input voltage and/or current damages the device. This clamp will not protect the device from an unregulated supply. If an unregulated supply is used, a series-connected fixed positive voltage regulator such as a UA78L15A is recommended. See the Absolute Maximum Ratings section for the limits on VCC voltage and current.

**ELECTRICAL CHARACTERISTICS (continued)**

over operating free-air temperature range  $-40^{\circ}\text{C} < T_A < 125^{\circ}\text{C}$ ,  $T_J = T_A$ ,  $V_{CC} = 12\text{ V}$ ,  $GND = 0\text{ V}$ ,  $R_{RT} = 75\text{ k}\Omega$ ,  $R_{DMX} = 68.1\text{ k}\Omega$ ,  $R_{RDM} = R_{SYN} = 100\text{ k}\Omega$ ,  $C_{CDR} = 2.2\text{ nF}$ ,  $C_{SS} = C_{VREF} = 0.1\text{ }\mu\text{F}$ ,  $C_{VCC} = 1\text{ }\mu\text{F}$ , (unless otherwise noted)

| SYMBOL                       | PARAMETER  | TEST CONDITIONS   | MIN  | TYP  | MAX  | UNITS         |
|------------------------------|--|---|------|------|------|---------------|
| <b>Clock Synchronization</b> |  |   |      |      |      |               |
| $V_{CDR}$                    | SYNC enable threshold                            | Measured at CDR (rising)  |      | 5    | 5.25 | V             |
|                              | SYNC propagation delay                           | $V_{CDR} = 6\text{ V}$ , Measured from RDM (rising) to GDx (rising) |      | 50   | 100  | ns            |
|                              | SYNC threshold (Rising)                          | $V_{CDR} = 6\text{ V}$ , Measured at RDM                            |      | 1.2  | 1.5  | V             |
|                              | SYNC threshold (Falling)                         | $V_{CDR} = 6\text{ V}$ , Measured at RDM                            | 0.4  | 0.7  |      |               |
|                              | SYNC pulses                                      | Positive pulse width  | 0.2  |      |      | $\mu\text{s}$ |
|                              |  | Maximum duty cycle <sup>(2)</sup>                                   |      | 50   |      | %             |
| <b>Voltage Amplifier</b>     |  |   |      |      |      |               |
|                              | VSENSE voltage                                   | In regulation, $T_A = 25^{\circ}\text{C}$                           | 2.97 | 3    | 3.03 | V             |
|                              | VSENSE voltage                                   | In regulation   | 2.94 | 3    | 3.06 |               |
|                              | VSENSE input bias current                        | In regulation   |      | 250  | 500  | nA            |
|                              | VAO high voltage                                 | $V_{SENSE} = 2.9\text{ V}$  | 4.8  | 5    | 5.2  | V             |
|                              | VAO low voltage                                  | $V_{SENSE} = 3.1\text{ V}$  |      | 0.05 | 0.50 |               |
| $g_{MV}$                     | VAO transconductance                             | $2.8\text{ V} < V_{SENSE} < 3.2\text{ V}$ , $VAO = 3\text{ V}$      |      | 70   |      | $\mu\text{S}$ |
|                              | VAO sink current, overdriven limit               | $V_{SENSE} = 3.5\text{ V}$ , $VAO = 3\text{ V}$                     |      | 30   |      | $\mu\text{A}$ |
|                              | VAO source current, overdriven                   | $V_{SENSE} = 2.5\text{ V}$ , $VAO = 3\text{ V}$ , $SS = 3\text{ V}$ |      | -30  |      |               |
|                              | VAO source current, overdriven limit + $I_{SRC}$ | $V_{SENSE} = 2.5\text{ V}$ , $VAO = 3\text{ V}$                     |      | -130 |      |               |
|                              | Slew-rate correction threshold                   | Measured as $V_{SENSE}$ (falling) / $V_{SENSE}$ (regulation)        | 92   | 93   | 95   | %             |
|                              | Slew-rate correction hysteresis                  | Measured at $V_{SENSE}$ (rising)                                    |      | 3    | 9    | mV            |
| $I_{SRC}$                    | Slew-rate correction current                     | Measured at VAO, in addition to VAO source current.                 |      | -100 |      | $\mu\text{A}$ |
|                              | Slew-rate correction enable threshold            | Measured at SS (rising)   |      | 4    |      | V             |
|                              | VAO discharge current                            | $V_{SENSE} = 0.5\text{ V}$ , $VAO = 1\text{ V}$                     |      | 10   |      | $\mu\text{A}$ |
| <b>Soft Start</b>            |  |   |      |      |      |               |
| $I_{SS}$                     | SS source current                                | $V_{SENSE} = 0.9\text{ V}$ , $SS = 1\text{ V}$                      |      | -10  |      | $\mu\text{A}$ |
|                              | Adaptive source current                          | $V_{SENSE} = 2.0\text{ V}$ , $SS = 1\text{ V}$                      |      | -1.5 | -2.5 | mA            |
|                              | Adaptive SS disable                              | Measured as $V_{SENSE} - SS$  | -30  | 0    | 30   | mV            |
|                              | SS sink current                                  | $V_{SENSE} = 0.5\text{ V}$ , $SS = 0.2\text{ V}$                    | 0.5  | 0.9  |      | mA            |

(2) Due to the influence of the synchronization pulse width on the programmability of the maximum PWM switching duty cycle ( $D_{MAX}$ ) it is recommended to minimize the synchronization signal's duty cycle.

**ELECTRICAL CHARACTERISTICS (continued)**

 over operating free-air temperature range  $-40^{\circ}\text{C} < T_A < 125^{\circ}\text{C}$ ,  $T_J = T_A$ ,  $V_{CC} = 12\text{ V}$ ,  $GND = 0\text{ V}$ ,  $R_{RT} = 75\text{ k}\Omega$ ,  $R_{DMX} = 68.1\text{ k}\Omega$ ,  $R_{RDM} = R_{SYN} = 100\text{ k}\Omega$ ,  $C_{CDR} = 2.2\text{ nF}$ ,  $C_{SS} = C_{VREF} = 0.1\text{ }\mu\text{F}$ ,  $C_{VCC} = 1\text{ }\mu\text{F}$ , (unless otherwise noted)

| SYMBOL                                | PARAMETER                        | TEST CONDITIONS   | MIN  | TYP  | MAX  | UNITS         |
|---------------------------------------|----------------------------------|---|------|------|------|---------------|
| <b>Over Voltage</b>                   |                                  |   |      |      |      |               |
| $V_{OVP}$                             | OVP threshold                    | Measured as $V_{SENSE}$ (rising) / $V_{SENSE}$ (regulation)     | 104  | 106  | 108  | %             |
|                                       | OVP hysteresis                   | Measured at $V_{SENSE}$ (falling)                               |      | 100  |      | mV            |
|                                       | OVP propagation delay            | Measured between $V_{SENSE}$ (rising) and $GDx$ (falling)       |      | 0.2  | 0.3  | $\mu\text{s}$ |
| <b>Zero-Power</b>                     |                                  |   |      |      |      |               |
| $V_{ZPWR}$                            | Zero-power detect threshold      | Measured at $VAO$ (falling)                                     | 0.65 | 0.75 |      | V             |
|                                       | Zero-power hysteresis            |   |      | 0.15 |      |               |
| <b>Multiplier</b>                     |                                  |   |      |      |      |               |
| $k_{MULT}$                            | Gain constant                    | $VAO \geq 1.5\text{ V}$ , $T_A = 25^{\circ}\text{C}$            | 16   | 17   | 18   | $\mu\text{A}$ |
|                                       |                                  | $VAO = 1.2\text{ V}$ , $T_A = 25^{\circ}\text{C}$               | 14.5 | 17.0 | 19.5 |               |
|                                       |                                  | $VAO \geq 1.5\text{ V}$   | 15   | 17   | 19   |               |
|                                       |                                  | $VAO = 1.2\text{ V}$  | 13   | 17   | 21   |               |
| $I_{IMO}$                             | Output current: zero             | $V_{INAC} = 0.9 V_{PK}$ , $VAO = 0.8\text{ V}$                  | -0.2 | 0    | 0.2  |               |
|                                       |                                  | $V_{INAC} = 0\text{ V}$ , $VAO = 5\text{ V}$                    | -0.2 | 0    | 0.2  |               |
| <b>Quantized Voltage Feed Forward</b> |                                  |   |      |      |      |               |
| $V_{LVL1}$                            | Level 1 threshold <sup>(3)</sup> | Measured at $V_{INAC}$ (rising)                                 | 0.6  | 0.7  | 0.8  | V             |
| $V_{LVL2}$                            | Level 2 threshold                |   |      | 1    |      |               |
| $V_{LVL3}$                            | Level 3 threshold                |   |      | 1.2  |      |               |
| $V_{LVL4}$                            | Level 4 threshold                |   |      | 1.4  |      |               |
| $V_{LVL5}$                            | Level 5 threshold                |   |      | 1.65 |      |               |
| $V_{LVL6}$                            | Level 6 threshold                |   |      | 1.95 |      |               |
| $V_{LVL7}$                            | Level 7 threshold                |   |      | 2.25 |      |               |
| $V_{LVL8}$                            | Level 8 threshold                |   |      | 2.6  |      |               |
| <b>Current Amplifiers</b>             |                                  |   |      |      |      |               |
|                                       | CAOx high voltage                |   | 5.75 | 6    |      | V             |
|                                       | CAOx low voltage                 |   |      |      | 0.1  |               |
| $g_{MC}$                              | CAOx transconductance            |   |      | 100  |      | $\mu\text{S}$ |
|                                       | CAOx sink current, overdriven    |   |      | 50   |      | $\mu\text{A}$ |
|                                       | CAOx source current, overdriven  |   |      | -50  |      |               |
|                                       | Input common mode range          |   | 0    |      | 3.6  | V             |
|                                       | Input offset voltage             |   | 0    | -8   | -20  |               |
|                                       | Phase mismatch                   | Measured as Phase A's input offset minus Phase B's input offset | -12  | 0    | 12   | mV            |
|                                       | CAOx pull-down current           | $V_{SENSE} = 0.5\text{ V}$ , $CAOx = 0.2\text{ V}$              | 0.5  | 0.9  |      | mA            |

(3) The Level 1 threshold represents the "zero-crossing detection" threshold above which  $V_{INAC}$  must rise to initiate a new input half-cycle, and below which  $V_{INAC}$  must fall to terminate that half-cycle.

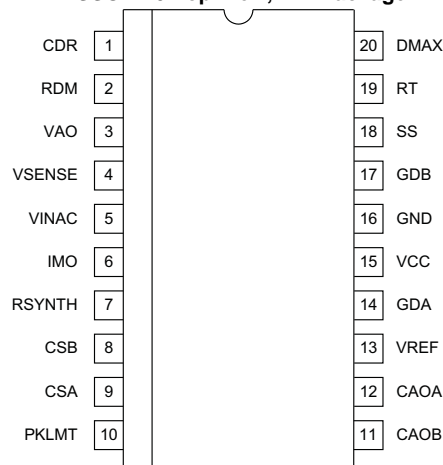
**ELECTRICAL CHARACTERISTICS (continued)**

over operating free-air temperature range  $-40^{\circ}\text{C} < T_A < 125^{\circ}\text{C}$ ,  $T_J = T_A$ ,  $V_{CC} = 12\text{ V}$ ,  $GND = 0\text{ V}$ ,  $R_{RT} = 75\text{ k}\Omega$ ,  $R_{DMX} = 68.1\text{ k}\Omega$ ,  $R_{RDM} = R_{SYN} = 100\text{ k}\Omega$ ,  $C_{CDR} = 2.2\text{ nF}$ ,  $C_{SS} = C_{VREF} = 0.1\text{ }\mu\text{F}$ ,  $C_{VCC} = 1\text{ }\mu\text{F}$ , (unless otherwise noted)

| SYMBOL                     | PARAMETER                               | TEST CONDITIONS   | MIN  | TYP   | MAX   | UNITS                        |
|----------------------------|---|---|------|-------|-------|------------------------------|
| <b>Current Synthesizer</b> |   |   |      |       |       |                              |
| $V_{RSYNTH}$               | Regulation voltage                      | $V_{SENSE} = 3\text{ V}$ , $V_{INAC} = 0\text{ V}$            | 2.91 | 3     | 3.09  | V                            |
|                            |   | $V_{SENSE} = 3\text{ V}$ , $V_{INAC} = 2.85\text{ V}$         | 0.10 | 0.15  | 0.20  |                              |
|                            | Synthesizer disable threshold           | Measured at RSYNTH (rising)                                   |      | 5     | 5.25  |                              |
|                            | VINAC input bias current                |   |      | 0.250 | 0.500 | $\mu\text{A}$                |
| <b>Peak Current Limit</b>  |   |   |      |       |       |                              |
|                            | Peak current limit threshold            | $PKLMT = 3.30\text{ V}$ , measured at CSx (rising)            | 3.27 | 3.3   | 3.33  | V                            |
|                            | Peak current limit propagation delay    | Measured between CSx (rising) and GDx (falling) edges         |      | 60    | 100   | ns                           |
| <b>PWM Ramp</b>            |   |   |      |       |       |                              |
| $V_{RMP}$                  | PWM ramp amplitude                      |   | 3.8  | 4.0   | 4.2   | V                            |
|                            | PWM ramp offset voltage                 | $T_A = 25^{\circ}\text{C}$ , $R_{RT} = 75\text{ k}\Omega$     | 0.65 | 0.7   |       |                              |
|                            | PWM ramp offset temperature coefficient |   |      | -2    |       | $\text{mV}/^{\circ}\text{C}$ |
| <b>Gate Drive</b>          |   |   |      |       |       |                              |
|                            | GDA, GDB output voltage, high, clamped  | $V_{CC} = 20\text{ V}$ , $C_{LOAD} = 1\text{ nF}$             | 11.5 | 13    | 15    | V                            |
|                            | GDA, GDB output voltage, High           | $C_{LOAD} = 1\text{ nF}$                                      | 10   | 10.5  |       |                              |
|                            | GDA, GDB output voltage, Low            | $C_{LOAD} = 1\text{ nF}$                                      |      | 0.2   | 0.3   |                              |
|                            | Rise time GDx                           | 1 V to 9 V, $C_{LOAD} = 1\text{ nF}$                          |      | 18    | 30    | ns                           |
|                            | Fall time GDx                           | 9 V to 1 V, $C_{LOAD} = 1\text{ nF}$                          |      | 12    | 25    |                              |
|                            | GDA, GDB output voltage, UVLO           | $V_{CC} = 0\text{ V}$ , $I_{GDA}$ , $I_{GDB} = 2.5\text{ mA}$ |      | 0.7   | 2     | V                            |
| <b>Thermal Shutdown</b>    |   |   |      |       |       |                              |
|                            | Thermal shutdown threshold              |   |      | 160   |       | $^{\circ}\text{C}$           |
|                            | Thermal shutdown recovery               |   |      | 140   |       |                              |

**DEVICE INFORMATION**

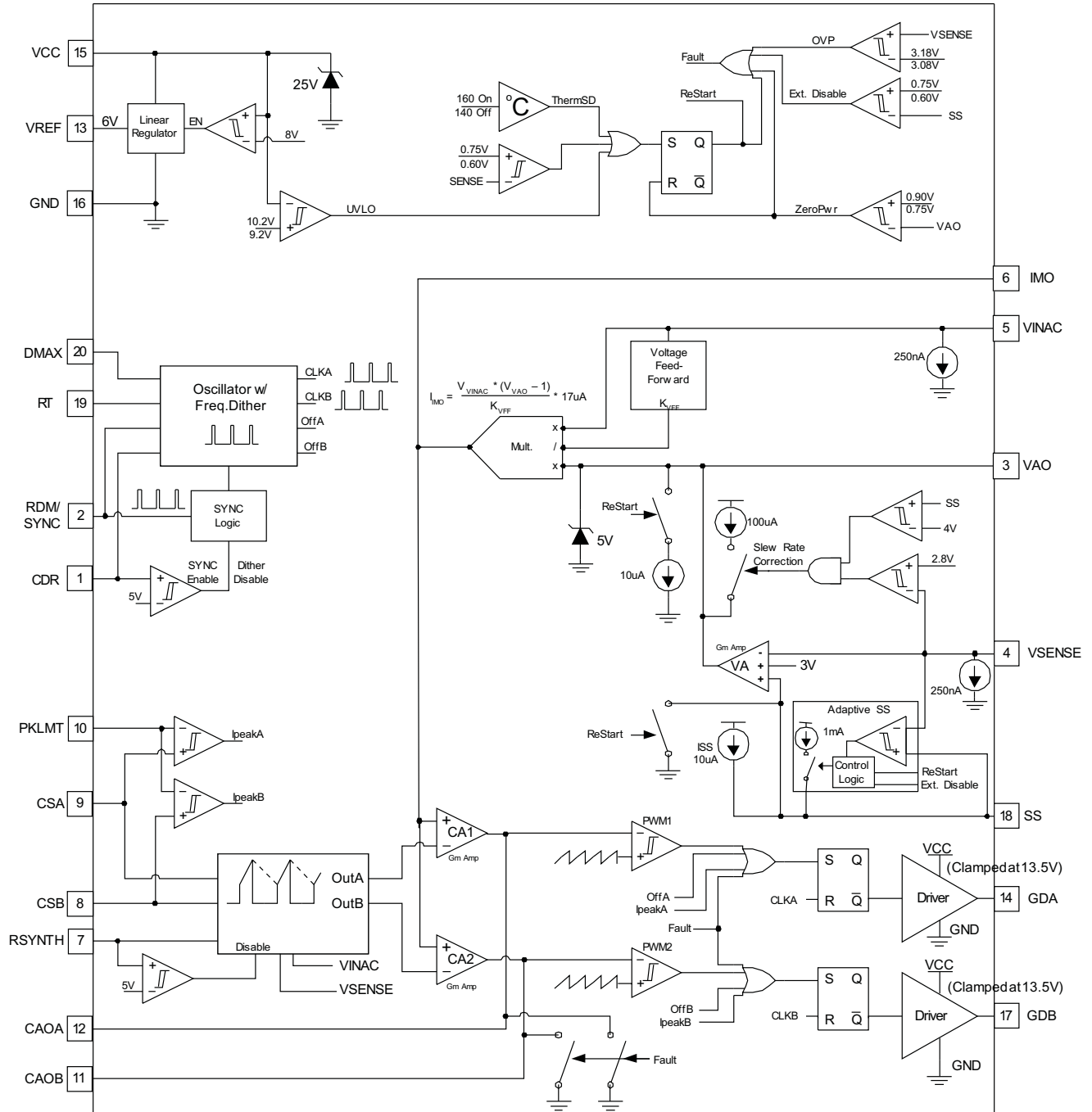
TSSOP-20 Top View, PW Package



**TERMINAL FUNCTIONS**

| NAME          | PIN # | I/O | DESCRIPTION   |
|---------------|-------|-----|---|
| CDR           | 1     | I   | <b>Dither Rate Capacitor.</b> Frequency-dithering timing pin. An external capacitor to GND programs the rate of oscillator dither. Connect the CDR pin to the VREF pin to disable dithering.  |
| RDM<br>(SYNC) | 2     | I   | <b>Dither Magnitude Resistor.</b> Frequency-dithering magnitude and external synchronization pin. An external resistor to GND programs the magnitude of oscillator frequency dither. When frequency dithering is disabled ( $CDR > 5\text{ V}$ ), the internal master clock will synchronize to positive edges presented on the RDM pin. Connect RDM to GND when dithering is disabled and synchronization is not desired.  |
| VAO           | 3     | O   | <b>Voltage Amplifier Output.</b> Output of transconductance voltage error amplifier. Internally connected to Multiplier input and Zero-Power comparator. Connect the voltage regulation loop compensation components between this pin and GND.  |
| VSENSE        | 4     | I   | <b>Output Voltage Sense.</b> Internally connected to the inverting input of the transconductance voltage error amplifier in addition to the positive terminal of the Current Synthesis difference amplifier. Also connected to the OVP, PFC Enable, and slew-rate comparators. Connect to PFC output with a resistor-divider network.   |
| VINAC         | 5     | I   | <b>Scaled AC Line Input Voltage.</b> Internally connected to the Multiplier and negative terminal of the Current Synthesis difference amplifier. Connect a resistor-divider network between $V_{IN}$ , VINAC, and GND identical to the PFC output divider network connected at VSENSE.  |
| IMO           | 6     | O   | <b>Multiplier Current Output.</b> Connect a resistor between this pin and GND to set the multiplier gain.   |
| RSYNTH        | 7     | I   | <b>Current Synthesis Down-Slope Programming.</b> Connect a resistor between this pin and GND to set the magnitude of the current synthesizer down-slope. Connecting RSYNTH to VREF will disable current synthesis and connect CSA and CSB directly to their respective current amplifiers.  |
| CSB           | 8     | I   | <b>Phase B Current Sense Input.</b> During the on-time of GDB, CSB is internally connected to the inverting input of Phase B's current amplifier through the current synthesis stage.   |
| CSA           | 9     | I   | <b>Phase A Current Sense Input.</b> During the on-time of GDA, CSA is internally connected to the inverting input of Phase A's current amplifier through the current synthesis stage.   |
| PKLMT         | 10    | I   | <b>Peak Current Limit Programming.</b> Connect a resistor-divider network between VREF and this pin to set the voltage threshold of the cycle-by-cycle peak current limiting comparators. Allows adjustment for desired $\Delta I_{LB}$ .   |
| CAOB          | 11    | O   | <b>Phase B Current Amplifier Output.</b> Output of phase B's transconductance current amplifier. Internally connected to the inverting input of phase B's PWM comparator for trailing-edge modulation. Connect the current regulation loop compensation components between this pin and GND.  |
| CAOA          | 12    | O   | <b>Phase A Current Amplifier Output.</b> Output of phase A's transconductance current amplifier. Internally connected to the inverting input of phase A's PWM comparator for trailing-edge modulation. Connect the current regulation loop compensation components between this pin and GND.  |
| VREF          | 13    | O   | <b>6-V Reference Voltage and Internal Bias Voltage.</b> Connect a 0.1- $\mu\text{F}$ ceramic bypass capacitor as close as possible to this pin and GND.   |
| GDA           | 14    | O   | <b>Phase A's Gate Drive.</b> This limited-current output is intended to connect to a separate gate-drive device suitable for driving the Phase A switching component(s). The output voltage is typically clamped to 13.5 V.   |
| VCC           | 15    | I   | <b>Bias Voltage Input.</b> Connect a 0.1- $\mu\text{F}$ ceramic bypass capacitor as close as possible to this pin and GND.  |
| GND           | 16    | I/O | <b>Device Ground Reference.</b> Connect all compensation and programming resistor and capacitor networks to this pin. Connect this pin to the system through a separate trace for high-current noise isolation.   |
| GDB           | 17    | O   | <b>Phase B's Gate Drive.</b> This limited-current output is intended to connect to a separate gate-drive device suitable for driving the Phase B switching component(s). The output voltage is typically clamped to 13.5 V.   |
| SS            | 18    | I   | <b>Soft-Start and External Fault Interface.</b> Connect a capacitor to GND on this pin to set the soft-start slew rate based on an internally-fixed 10- $\mu\text{A}$ current source. The regulation reference voltage for VSENSE is clamped to $V_{SS}$ until $V_{SS}$ exceeds 3 V. Upon recovery from certain fault conditions a 1-mA current source is present at the SS pin until the SS voltage equals the VSENSE voltage. Pulling the SS pin below 0.6 V immediately disables both GDA and GDB outputs. |
| RT            | 19    | I   | <b>Timing Resistor.</b> Oscillator frequency programming pin. A resistor to GND sets the running frequency of the internal oscillator.  |
| DMAX          | 20    | I   | <b>Maximum Duty-Cycle Resistor.</b> Maximum PWM duty-cycle programming pin. A resistor to GND sets the PWM maximum duty-cycle based on the ratio of $R_{DMX}/R_{RT}$ .  |

Functional Block Diagram





### TYPICAL CHARACTERISTICS

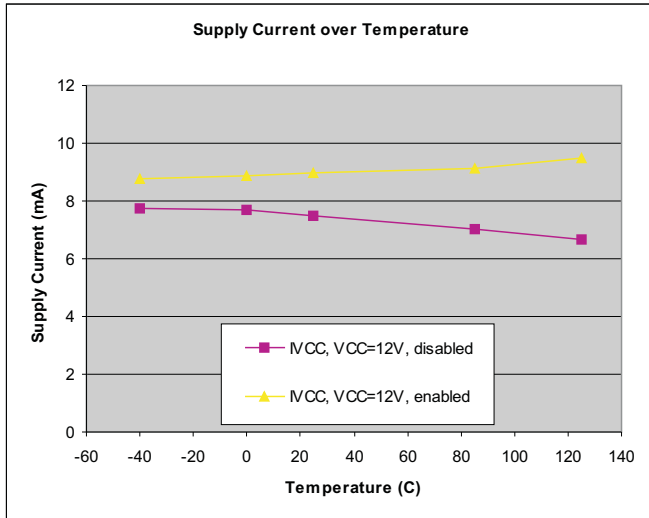


Figure 1.

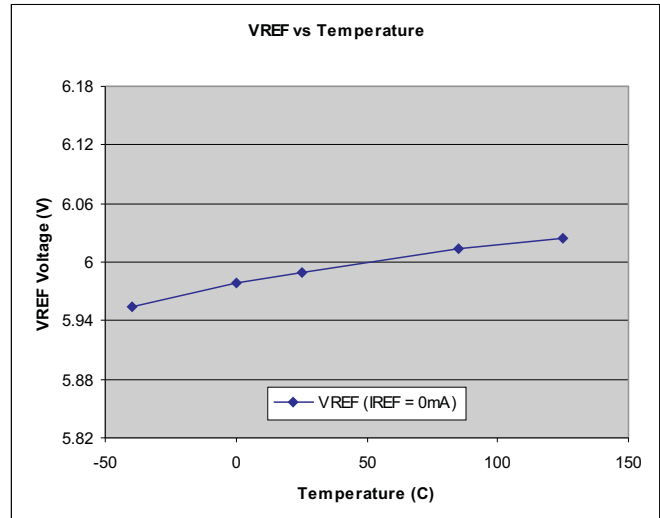


Figure 2.

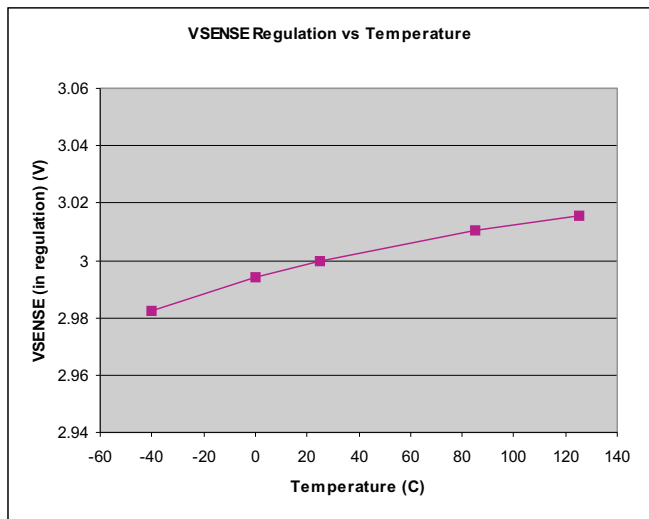


Figure 3.

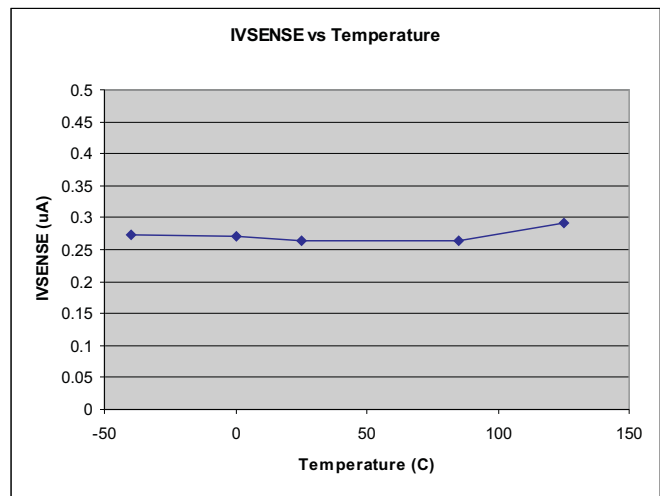


Figure 4.

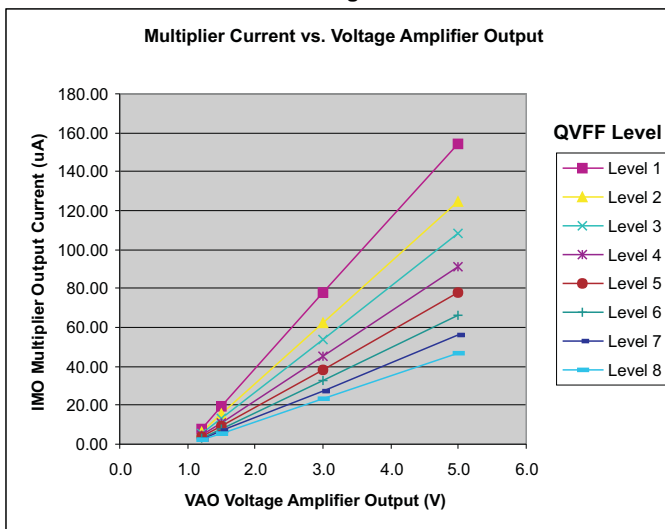


Figure 5.

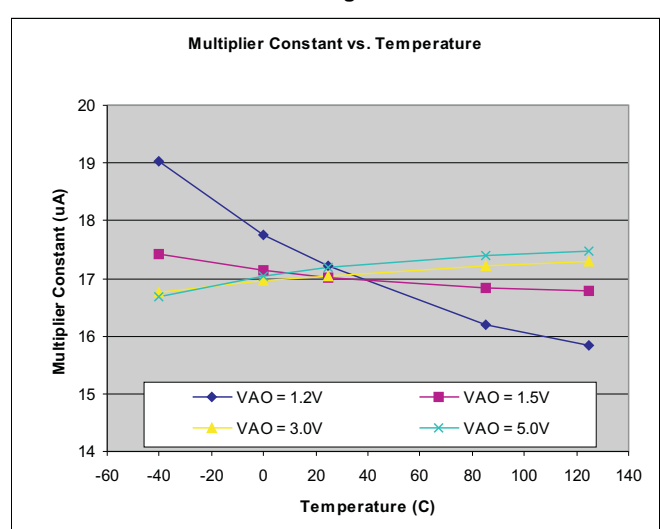


Figure 6.

TYPICAL CHARACTERISTICS (continued)

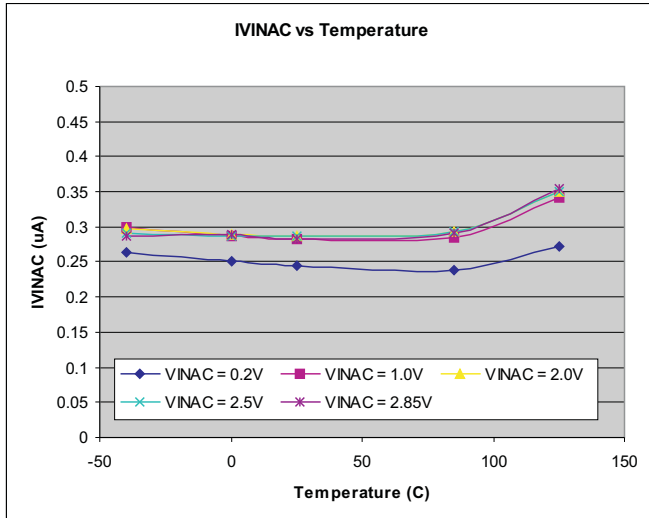


Figure 7.

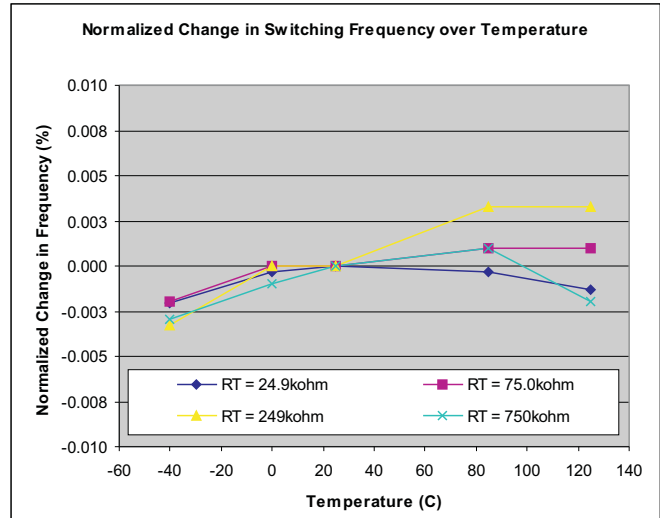


Figure 8.

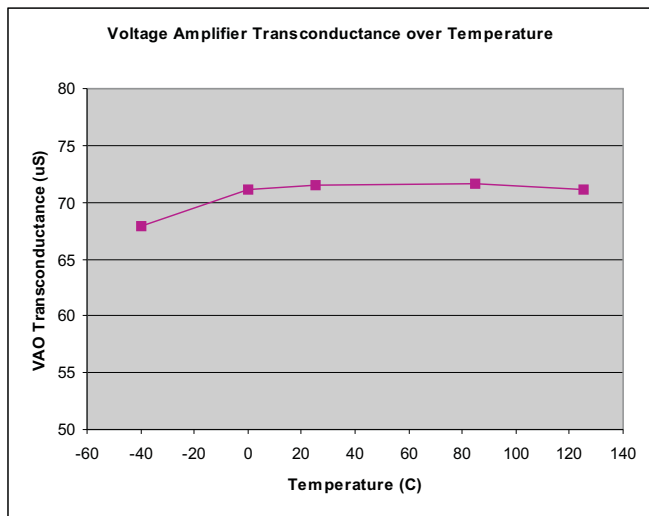


Figure 9.

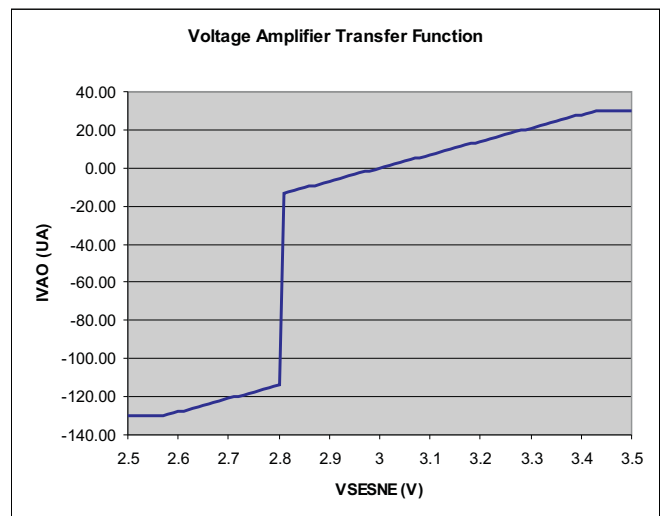
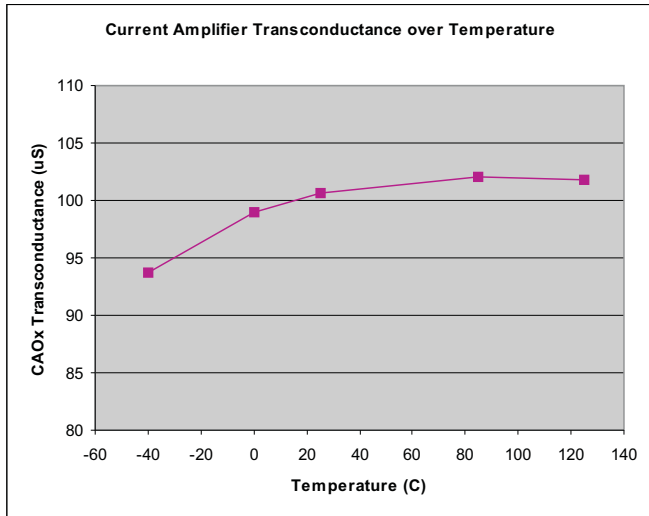
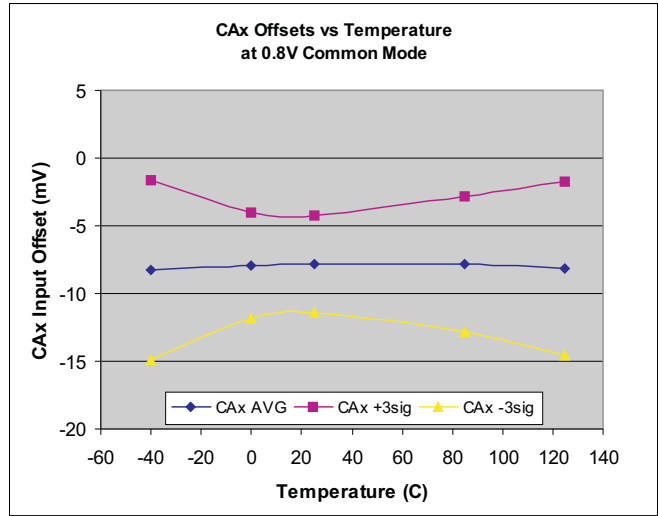


Figure 10.

**TYPICAL CHARACTERISTICS (continued)**



**Figure 11.**



**Figure 12.**

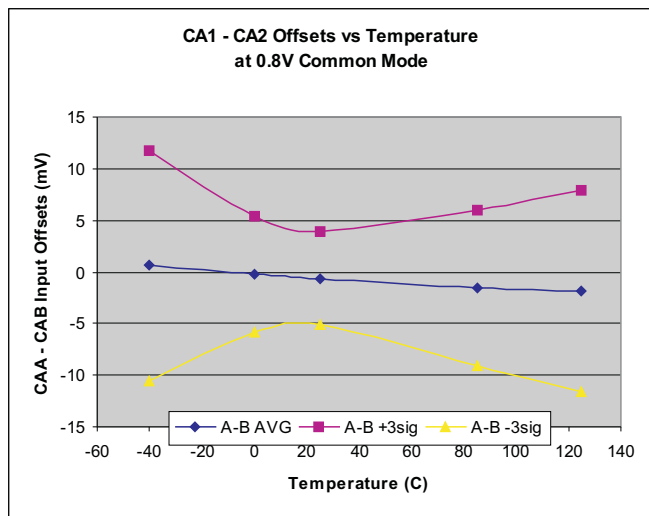


**Figure 13.**

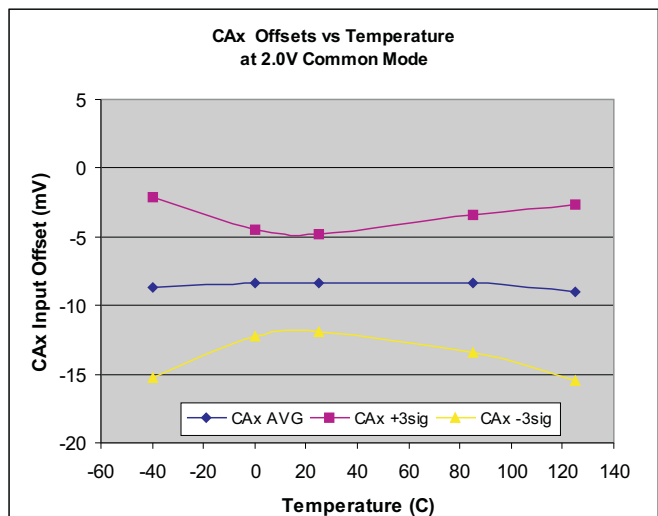


**Figure 14.**

TYPICAL CHARACTERISTICS (continued)

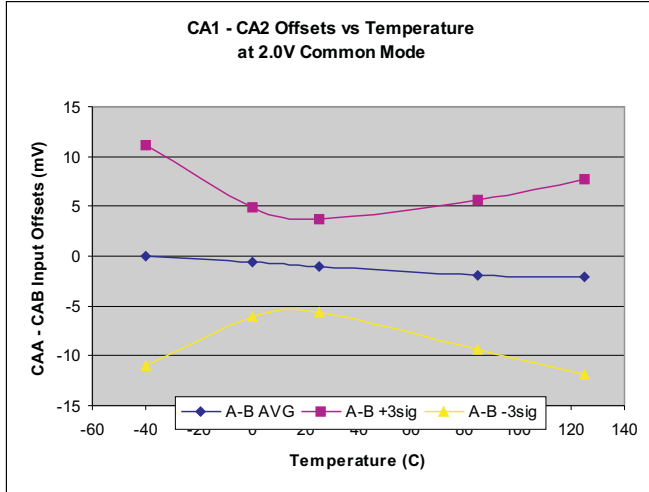


Figure 15.

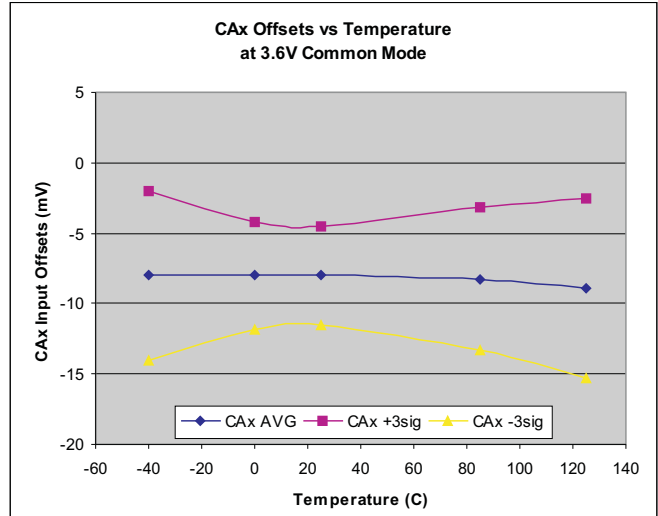


Figure 16.

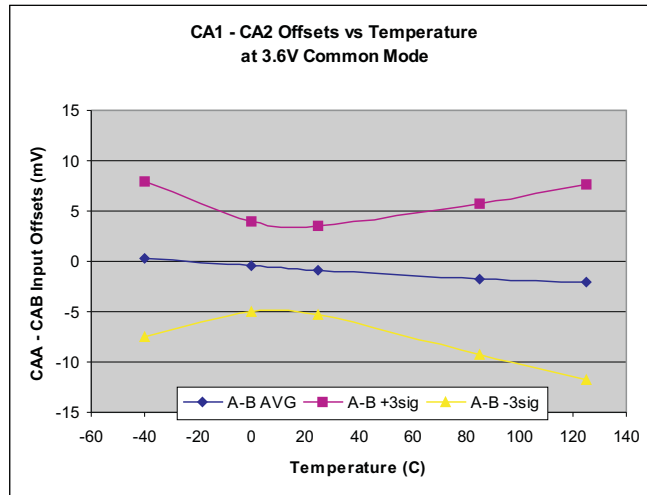


Figure 17.

## APPLICATION INFORMATION

### THEORY OF OPERATION

#### Interleaving

One of the main benefits from the 180° interleaving of phases is significant reductions in the high-frequency ripple components of both the input current and the current into the output capacitor of the PFC pre-regulator. Compared to that of a single-phase PFC stage of equal power, the reduced ripple on the input current eases the burden of filtering conducted-EMI noise and helps reduce the EMI filter and  $C_{IN}$  sizes. Additionally, reduced high-frequency ripple current into the PFC output capacitor,  $C_{OUT}$ , helps to reduce its size and cost. Furthermore, with reduced ripple and average current in each phase, the boost inductor size can be smaller than in a single-phase design [1].

Ripple current reduction due to interleaving is often referred to as “ripple cancellation”, but strictly speaking, the peak-to-peak ripple is completely cancelled only at 50% duty-cycle in a 2-phase system. At duty-cycles other than 50%, ripple reduction occurs in the form of partial cancellation due to the superposition of the individual phase currents. Nevertheless, compared to the ripple currents of an equivalent single-phase PFC pre-regulator, those of a 2-phase interleaved design are extraordinarily smaller [1]. Independent of ripple cancellation, the frequency of the interleaved ripple, at both the input and output, is  $2 \times f_{PWM}$ .

On the input, 180° interleaving reduces the peak-to-peak ripple amplitude to 1/2 or less of the ripple amplitude of the equivalent single-phase current.

On the output, 180° interleaving reduces the rms value of the PFC-generated ripple current in the output capacitor by a factor of slightly more than  $\sqrt{2}$ , for PWM duty-cycles > 50%.

This can be seen in the following derivations, adapting the method by Erickson [2].

In a single-phase PFC pre-regulator, the total rms capacitor current contributed by the PFC stage at all duty-cycles can be shown to be approximated by:

$$i_{CRMS1\phi} = \left( \frac{I_O}{\eta} \right) \sqrt{\left( \left( \frac{16V_O}{3\pi V_M} \right) - \ln^2 \right)} \quad (1)$$

In a dual-phase interleaved PFC pre-regulator, the total rms capacitor current contributed by the PFC stage for  $D > 50\%$  can be shown to be approximated by:

$$i_{CRMS2\phi} = \left( \frac{I_O}{\eta} \right) \sqrt{\left( \left( \frac{16V_O}{6\pi V_M} \right) - \ln^2 \right)} \quad (2)$$

In these equations,  $I_O$  = average PFC output load current,  $V_O$  = average PFC output voltage,  $V_M$  = peak of the input ac-line voltage, and  $\eta$  = efficiency of the PFC stage at these conditions. It can be seen that the quantity under the radical for  $i_{CRMS2\phi}$  is slightly smaller than 1/2 of that under the radical for  $i_{CRMS1\phi}$ . The rms currents shown contain both the low-frequency and the high-frequency components of the PFC output current. Interleaving reduces the high-frequency component, but not the low-frequency component.

### Programming the PWM Frequency and Maximum Duty-Cycle Clamp

The PWM frequency and maximum duty-cycle clamps for both GDx outputs of the UCC28070 are set through the selection of the resistors connected to the RT and DMAX pins, respectively. The selection of the RT resistor ( $R_{RT}$ ) directly sets the PWM frequency ( $f_{PWM}$ ).

$$R_{RT} (k\Omega) = \frac{7500}{f_{PWM} (kHz)} \quad (3)$$

Once  $R_{RT}$  has been determined, the  $D_{MAX}$  resistor ( $R_{DMX}$ ) may be derived.

$$R_{DMX} = R_{RT} \times (2 \times D_{MAX} - 1) \quad (4)$$

where  $D_{MAX}$  is the desired maximum PWM duty-cycle.

### Frequency Dithering (Magnitude and Rate)

Frequency dithering refers to modulating the switching frequency to achieve a reduction in conducted-EMI noise beyond the capability of the line filter alone. The UCC28070 implements a triangular modulation method which results in equal time spent at every point along the switching frequency range. This total range from minimum to maximum frequency is defined as the dither magnitude, and is centered around the nominal switching frequency  $f_{PWM}$  set with  $R_{RT}$ . For example, a dither magnitude of 20 kHz on a nominal  $f_{PWM}$  of 100 kHz results in a frequency range of 100 kHz  $\pm$ 10 kHz. Furthermore, the programmed duty-cycle clamp set by  $R_{DMX}$  remains constant at the programmed value across the entire range of the frequency dithering.

The rate at which  $f_{PWM}$  traverses from one extreme to the other and back again is defined as the dither rate. For example, a dither rate of 1 kHz would linearly modulate the nominal frequency from 110 kHz to 90 kHz to 110 kHz once every millisecond. A good initial design target for dither magnitude is  $\pm$ 10% of  $f_{PWM}$ . Most boost components can tolerate such a spread in  $f_{PWM}$ . The designer can then iterate around there to find the best compromise between EMI reduction, component tolerances, and loop stability.

The desired dither magnitude is set by a resistor from the RDM pin to GND, of value calculated by the following equation:

$$R_{RDM} (k\Omega) = \frac{937.5}{f_{DM} (kHz)} \quad (5)$$

Once the value of  $R_{RDM}$  is determined, the desired dither rate may be set by a capacitor from the CDR pin to GND, of value calculated by the following equation:

$$C_{CDR} (pF) = 66.7 \times \left( \frac{R_{RDM} (k\Omega)}{f_{DR} (kHz)} \right) \quad (6)$$

Frequency dithering may be fully disabled by forcing the CDR pin  $>$  5 V or by connecting it to VREF (6 V) and connecting the RDM pin directly to GND. (If populated, the relatively high impedance of the RDM resistor may allow system switching noise to couple in and interfere with the controller timing functions if not bypassed with a low impedance path when dithering is disabled.)

If an external frequency source is used to synchronize  $f_{PWM}$  and frequency dithering is desired, the external frequency source must provide the dither magnitude and rate functions as the internal dither circuitry is disabled to prevent undesired performance during synchronization. (See following section for more details.)

## External Clock Synchronization

The UCC28070 has also been designed to be easily synchronized to almost any external frequency source. By disabling frequency dithering (pulling CDR > 5 V), the UCC28070's SYNC circuitry is enabled permitting the internal oscillator to be synchronized with pulses presented on the RDM pin. In order to ensure a precise 180 degree phase shift is maintained between the GDA and GDB outputs, the frequency ( $f_{SYNC}$ ) of the pulses presented at the RDM pin needs to be at twice the desired  $f_{PWM}$ . For example, if a 100-kHz switching frequency is desired, the  $f_{SYNC}$  should be 200 kHz.

$$f_{PWM} = \frac{f_{SYNC}}{2} \quad (7)$$

In order to ensure the internal oscillator does not interfere with the SYNC function,  $R_{RT}$  should be sized to set the internal oscillator frequency at least 10% below the  $f_{SYNC}$ . It must be noted that the PWM modulator gain will be reduced by a factor equivalent to the scaled  $R_{RT}$  due to a direct correlation between the PWM ramp current and  $R_{RT}$ . Adjustments to the current loop gains should be made accordingly.

It must also be noted that the maximum duty cycle clamp programmability is affected during external synchronization. The internal timing circuitry responsible for setting the maximum duty cycle is initiated on the falling edge of the synchronization pulse. Therefore, the selection of  $R_{DMX}$  becomes dependent on the synchronization pulse width ( $t_{SYNC}$ ).

$$t_{OFF} = \frac{2 \times (1 - D_{MAX})}{f_{SYNC}} \quad (8)$$

For use in  $R_{DMX}$  equation immediately below.

$$R_{DMX} (k\Omega) = \frac{1}{f_{SYNC}} \frac{t_{SYNC} - t_{OFF}}{66 \times 10^{-9}} \quad (9)$$

Consequently to minimize the impact of the  $t_{SYNC}$  it is clearly advantageous to utilize the smallest synchronization pulse width feasible.

$$R_{RT} (k\Omega) = 1.1 \times \frac{15000}{f_{SYNC} (kHz)} \quad (10)$$

$$f_{SYN(maxD)} \leq 0.9 \times (2 \times D_{MAX} - 1) \quad (11)$$

### NOTE:

When external synchronization is used, a propagation delay of approximately 50 ns to 100 ns exists between internal timing circuits and the SYNC signal's falling edge, which may result in reduced off-time at the highest of switching frequencies. Therefore,  $R_{DMX}$  should be adjusted downward slightly by  $(T_{SYNC} - 0.1 \mu s) / T_{SYNC}$  to compensate. At lower SYNC frequencies, this delay becomes an insignificant fraction of the PWM period, and can be neglected.

## Multi-phase Operation

External synchronization also facilitates using more than 2 phases for interleaving. Multiple UCC28070s can easily be paralleled to add an even number of additional phases for higher-power applications. With appropriate phase-shifting of the synchronization signals, even more input and output ripple current cancellation can be obtained. (An odd number of phases can be accommodated if desired, but the ripple cancellation would not be optimal.) For 4-, 6-, or any  $2 \times n$ -phases (where  $n$  = the number of UCC28070 controllers), each controller should receive a SYNC signal which is  $360/n$  degrees out of phase with each other. For a 4-phase application interleaving with two controllers, SYNC1 should be  $180^\circ$  out of phase with SYNC2 for optimal ripple cancellation. Similarly for a 6-phase system, SYNC1, SYNC2, and SYNC3 should be  $120^\circ$  out of phase with each other for optimal ripple cancellation.

In a multi-phase interleaved system, each current loop is independent and treated separately, however there is only one common voltage loop. To maintain a single control loop, all VSENSE, VINAC, SS, IMO and VAO signals are paralleled, respectively between the  $n$  controllers. Where current-source outputs are combined (SS, IMO, VAO), the calculated load impedances must be adjusted by  $1/n$  to maintain the same performance as with a single controller.

Figure 18 illustrates the paralleling of two controllers for a 4-phase  $90^\circ$ -interleaved PFC system.

## VSENSE and VINAC Resistor Configuration

The primary purpose of the VSENSE input is to provide the voltage feedback from the output to the voltage control loop. Thus, a traditional resistor-divider network needs to be sized and connected between the output capacitor and the VSENSE pin to set the desired output voltage based on the 3-V regulation voltage on VSENSE.

A unique aspect of the UCC28070 is the need to place the same resistor-divider network on the  $V_{IN}$  side of the inductor to the VINAC pin. This provides the scaled input voltage monitoring needed for the linear multiplier and current synthesizer circuitry. It is not required that the actual resistance of the VINAC network be identical to the VSENSE network, but it is necessary that the attenuation ( $k_R$ ) of the two divider networks be equivalent for proper PFC operation.

$$k_R = \frac{R_B}{(R_A + R_B)} \quad (12)$$

In noisy environments, it may be beneficial for small filter capacitors to be applied to the VSENSE and VINAC inputs to avoid the destabilizing effects of excessive noise on these inputs. If applied, the RC time-constant should not exceed  $100\mu\text{s}$  on the VSENSE input to avoid significant delay in the output transient response. The RC time-constant should also not exceed  $100\mu\text{s}$  on the VINAC input to avoid degrading of the wave-shape zero-crossings. Usually, a time constant of  $3/f_{\text{PWM}}$  is adequate to filter out typical noise on VSENSE and VINAC. Some design and test iteration may be required to find the optimal amount of filtering required in a particular application.

## VSENSE and VINAC Open Circuit Protection

Both the VSENSE and VINAC pins have been designed with an internal 250-nA current sink to ensure that in the event of an open circuit at either pin, the voltage is not left undefined, and the UCC28070 remains in a “safe” operating mode.



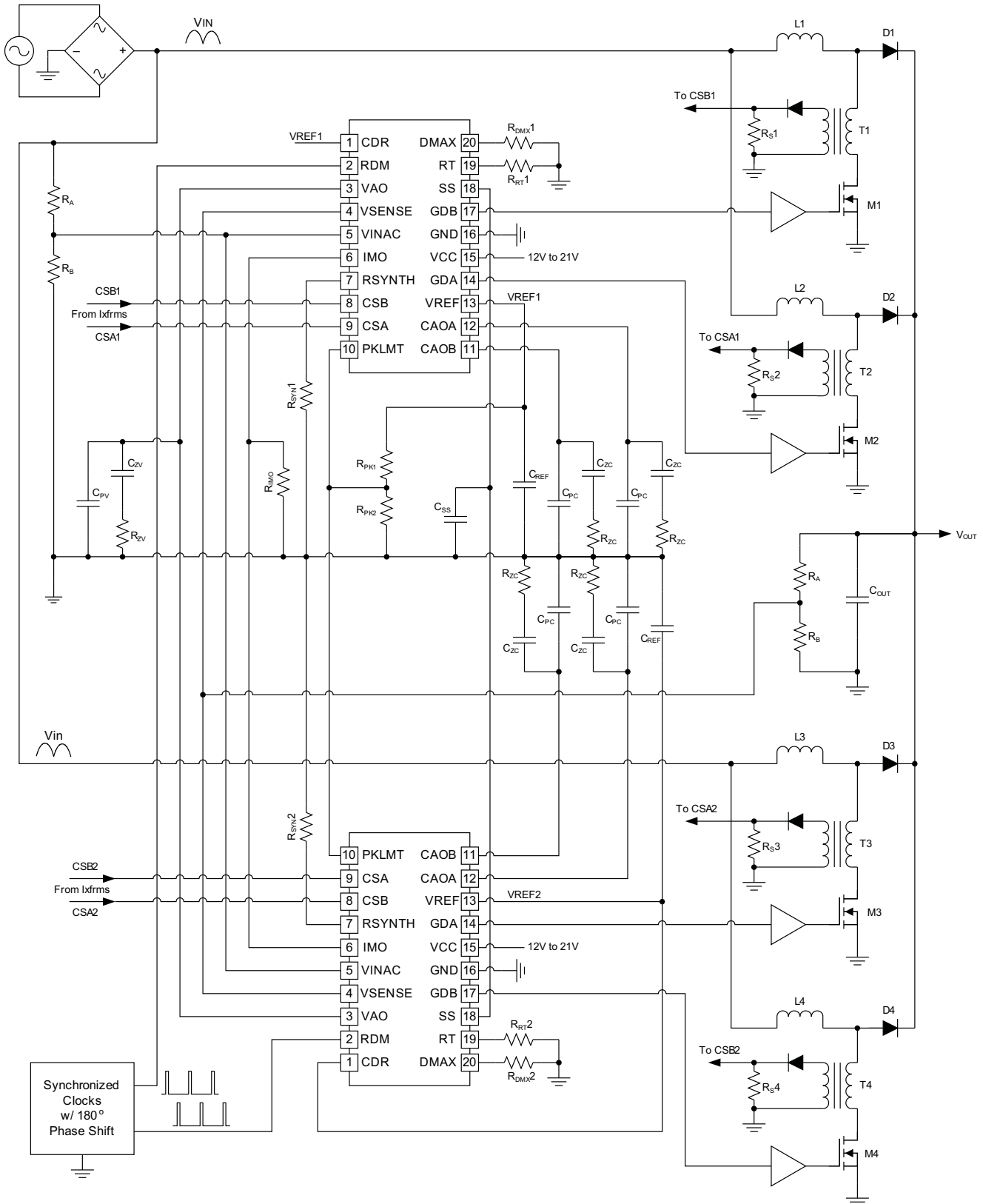


**Figure 18. Simplified Four-Phase Application Diagram Using Two UCC28070**

**Current Synthesizer**

One of the most prominent innovations in the UCC28070 design is the current synthesizer circuitry that synchronously monitors the instantaneous inductor current through a combination of on-time sampling and off-time down-slope emulation.

During the on-time of the GDA and GDB outputs, the inductor current is recorded at the CSA and CSB pins respectively via the current transformer network in each output phase. Meanwhile, the continuous monitoring of the input and output voltage via the VINAC and VSENSE pins permits the UCC28070 to internally recreate the inductor current’s down-slope during each output’s respective off-time. Through the selection of the RSYNTH resistor ( $R_{SYN}$ ), based on the equation below, the internal response may be adjusted to accommodate the wide range of inductances expected across the wide array of applications.

During inrush surge events at power-up and ac drop-out recovery,  $VSENSE < VINAC$ , so the synthesized down slope becomes zero. In this case, the synthesized inductor current will remain above the IMO reference and the current loop drives the duty cycle to zero. This avoids excessive stress on the MOSFETS during the surge event. Once VINAC falls below VSENSE the duty cycle increases until steady-state operation resumes.

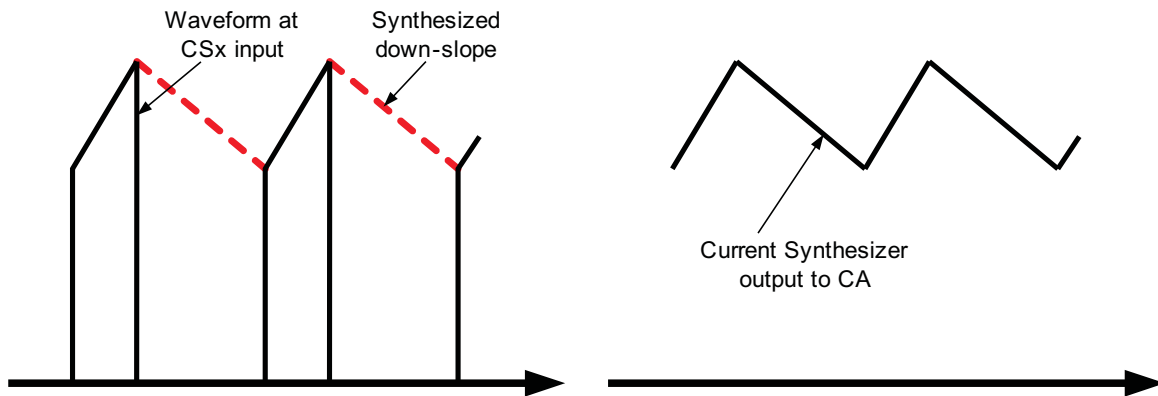


**Figure 19. Inductor Current’s Down Slope**

$$R_{SYN} (k\Omega) = \frac{(10 \times N_{CT} \times L_B (\mu H) \times k_R)}{R_S (\Omega)} \tag{13}$$

**Variables**

- $L_B$  = Nominal Zero-Bias Boost Inductance ( $\mu H$ ),
- $R_S$  = Sense Resistor ( $\Omega$ ),
- $N_{CT}$  = Current-sense Transformer turns ratio,
- $k_R = R_B / (R_A + R_B)$  = the resistor-divider attenuation at the VSENSE and VINAC pins.

### Programmable Peak Current Limit

The UCC28070 has been designed with a programmable cycle-by-cycle peak current limit dedicated to disabling either GDA or GDB output whenever the corresponding current-sense input (CSA or CSB respectively) rises above the voltage established on the PKLMT pin. Once an output has been disabled via the detection of peak current limit, the output remains disabled until the next clock cycle initiates a new PWM period. The programming range of the PKLMT voltage extends to upwards of 4 V to permit the full utilization of the 3-V average current sense signal range, however it should be noted that the linearity of the current amplifiers begin to compress above 3.6 V.

A resistor-divider network from VREF to GND can easily program the peak current limit voltage on PKLMT, provided the total current out of VREF is less than 2 mA to avoid drooping of the 6-V VREF voltage. A load of less than 0.5 mA is suggested, but if the resistance on PKLMT is very high, a small filter capacitor on PKLMT is recommended to avoid operational problems in high-noise environments.

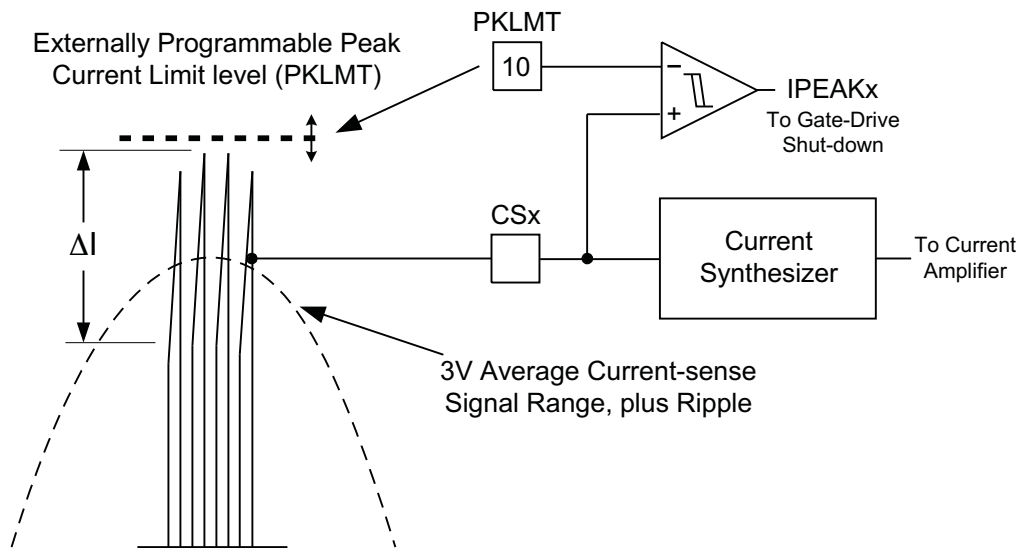


**Figure 20. Externally Programmable Peak Current Limit**

### Linear Multiplier

The multiplier of the UCC28070 generates a reference current which represents the desired wave shape and proportional amplitude of the ac input current. This current is converted to a reference voltage signal by the  $R_{IMO}$  resistor, which is scaled in value to match the voltage of the current-sense signals. The instantaneous multiplier current is dependent upon the rectified, scaled input voltage  $V_{VINAC}$  and the voltage-error amplifier output  $V_{VAO}$ . The  $V_{VINAC}$  signal conveys three pieces of information to the multiplier:

1. The overall wave-shape of the input voltage (typically sinusoidal),
2. The instantaneous input voltage magnitude at any point in the line cycle,
3. The rms level of the input voltage.

The  $V_{VAO}$  signal represents the total output power of the PFC pre-regulator.

A major innovation in the UCC28070 multiplier architecture is the internal quantized  $V_{RMS}$  feed-forward ( $Q_{VFF}$ ) circuitry, which eliminates the requirement for external filtering of the VINAC signal and the subsequent slow response to transient line variations. A unique circuit algorithm detects the transition of the peak of  $V_{VINAC}$  through seven thresholds and generates an equivalent VFF level centered within the eight  $Q_{VFF}$  ranges. The boundaries of the ranges expand with increasing  $V_{IN}$  to maintain an approximately equal-percentage delta between levels. These eight  $Q_{VFF}$  levels are spaced to accommodate the full “universal” line range of 85 V-265  $V_{RMS}$ .

A great benefit of the  $Q_{VFF}$  architecture is that the fixed  $k_{VFF}$  factors eliminate any contribution to distortion of the multiplier output, unlike an externally-filtered VINAC signal which unavoidably contains 2nd-harmonic distortion components. Furthermore, the  $Q_{VFF}$  algorithm allows for rapid response to both increasing and decreasing changes in input rms voltage so that disturbances transmitted to the PFC output are minimized. 5% hysteresis in the level thresholds help avoid “chattering” between  $Q_{VFF}$  levels for  $V_{VINAC}$  voltage peaks near a particular threshold or containing mild ringing or distortion. The  $Q_{VFF}$  architecture requires that the input voltage be largely sinusoidal, and relies on detecting zero-crossings to adjust  $Q_{VFF}$  downward on decreasing input voltage. Zero-crossings are defined as  $V_{VINAC}$  falling below 0.7 V for at least 50  $\mu s$  typically.

Table 1 reflects the relationship between the various VINAC peak voltages and the corresponding  $k_{VFF}$  terms for the multiplier equation.

**Table 1. VINAC Peak Voltages**

| LEVEL | $V_{VINAC}$ PEAK VOLTAGE                           | $k_{VFF}$ ( $V^2$ ) | $V_{IN}$ PEAK VOLTAGE <sup>(1)</sup> |
|-------|--|---------------------|--------------------------------------|
| 8     | $2.60\text{ V} \leq V_{VINAC(pk)}$                 | 3.857               | > 345 V                              |
| 7     | $2.25\text{ V} \leq V_{VINAC(pk)} < 2.60\text{ V}$ | 2.922               | 300 V to 345 V                       |
| 6     | $1.95\text{ V} \leq V_{VINAC(pk)} < 2.25\text{ V}$ | 2.199               | 260 V to 300 V                       |
| 5     | $1.65\text{ V} \leq V_{VINAC(pk)} < 1.95\text{ V}$ | 1.604               | 220 V to 260 V                       |
| 4     | $1.40\text{ V} \leq V_{VINAC(pk)} < 1.65\text{ V}$ | 1.156               | 187 V to 220 V                       |
| 3     | $1.20\text{ V} \leq V_{VINAC(pk)} < 1.40\text{ V}$ | 0.839               | 160 V to 187 V                       |
| 2     | $1.00\text{ V} \leq V_{VINAC(pk)} < 1.20\text{ V}$ | 0.600               | 133 V to 160 V                       |
| 1     | $V_{VINAC(pk)} \leq 1.00\text{ V}$                 | 0.398               | < 133 V                              |

(1) The  $V_{IN}$  peak voltage boundary values listed above are calculated based on a 400-V PFC output voltage and the use of a matched resistor-divider network ( $k_R = 3\text{ V}/400\text{ V} = 0.0075$ ) on VINAC and VSENSE (as required for current synthesis). When  $V_{OUT}$  is designed to be higher or lower than 400 V,  $k_R = 3\text{ V}/V_{OUT}$ , and the  $V_{IN}$  peak voltage boundary values for each  $Q_{VFF}$  level adjust to  $V_{VINAC(pk)}/k_R$ .

The multiplier output current  $I_{IMO}$  for any line and load condition can thus be determined by the equation

$$I_{IMO} = \frac{17\mu A \times (V_{VINAC}) \times (V_{VAO} - 1)}{k_{VFF}} \quad (14)$$

Because the  $k_{VFF}$  value represents the scaled  $V_{RMS}^2$  at the center of a level,  $V_{VAO}$  will adjust slightly upwards or downwards when  $V_{INACpk}$  is either lower or higher than the center of the  $Q_{VFF}$  voltage range to compensate for the difference. This is automatically accomplished by the voltage loop control when  $V_{IN}$  varies, both within a level and after a transition between levels.

The output of the voltage-error amplifier VAO is clamped at 5.0 V, which represents the maximum PFC output power. This value is used to calculate the maximum reference current at the IMO pin, and sets a limit for the maximum input power allowed (and, as a consequence, limits maximum output power).

Unlike a continuous  $V_{FF}$  situation, where maximum input power is a fixed power at any  $V_{RMS}$  input, the discrete  $Q_{VFF}$  levels permit a variation in maximum input power within limited boundaries as the input  $V_{RMS}$  varies within each level.

The lowest maximum power limit occurs at the VINAC voltage of 0.76 V, while the highest maximum power limit occurs at the increasing threshold from level-1 to level-2. This pattern repeats at every level transition threshold, keeping in mind that decreasing thresholds are 95% of the increasing threshold values. Below  $V_{INAC} = 0.76$  V,  $P_{IN}$  is always less than  $P_{IN(max)}$ , falling linearly to zero with decreasing input voltage.

For example, to design for the lowest maximum power allowable, determine the maximum steady-state (average) output power required of the PFC pre-regulator and add some additional percentage to account for line drop-out recovery power (to recharge  $C_{OUT}$  while full load power is drawn) such as 10% or 20% of  $P_{OUT(max)}$ . Then apply the expected efficiency factor to find the lowest maximum input power allowable:

$$P_{IN(max)} = \frac{1.10 \times P_{OUT(max)}}{\eta} \quad (15)$$

At the  $P_{IN(max)}$  design threshold,  $V_{VINAC} = 0.76$  V, hence  $Q_{VFF} = 0.398$  and input  $V_{AC} = 73 V_{RMS}$  (accounting for 2-V bridge-rectifier drop) for a nominal 400-V output system.

$$\text{Thus } I_{IN(rms)} = \frac{P_{IN(max)}}{73V_{RMS}}, \text{ and } I_{IN(pk)} = 1.414 \times I_{IN(rms)} \quad (16)$$

This  $I_{IN(pk)}$  value represents the combined average current through the boost inductors at the peak of the line voltage. Each inductor current is detected and scaled by a current-sense transformer (CT). Assuming equal currents through each interleaved phase, the signal voltage at each current sense input pin (CSA and CSB) is developed across a sense resistor selected to generate ~3 V based on  $(1/2) \times I_{IN(pk)} \times R_S/N_{CT}$ , where  $R_S$  is the current sense resistor and  $N_{CT}$  is the CT turns-ratio.

$I_{IMO}$  is then calculated at that same lowest maximum-power point, as

$$I_{IMO(max)} = 17 \mu A \times \frac{(0.76V)(5V - 1V)}{0.398} = 130 \mu A \quad (17)$$

$R_{IMO}$  is selected such that:

$$R_{IMO} \times I_{IMO(max)} = \left(\frac{1}{2}\right) \times I_{IN(pk)} \times \frac{R_S}{N_{CT}} \quad (18)$$

Therefore:

$$R_{IMO} = \frac{\left(\left(\frac{1}{2}\right) \times I_{IN(pk)} \times R_S\right)}{\left(N_{CT} \times I_{IMO(max)}\right)} \quad (19)$$

At the increasing side of the level-1 to level-2 threshold, it should be noted that the IMO current would allow higher input currents at low-line:

$$I_{IMO(L1-L2)} = 17 \mu A \times \frac{(1.0V)(5V - 1V)}{0.398} = 171 \mu A \quad (20)$$

However, this current may easily be limited by the programmable peak current limiting (PKLMT) feature of the UCC28070 if required by the power stage design.

The same procedure can be used to find the lowest and highest input power limits at each of the  $Q_{VFF}$  level transition thresholds. At higher line voltages, where the average current with inductor ripple is traditionally below the PKLMT threshold, the full variation of maximum input power will be seen, but the input currents will inherently be below the maximum acceptable current levels of the power stage.

The performance of the multiplier in the UCC28070 has been significantly enhanced when compared to previous generation PFC controllers, with high linearity and accuracy over most of the input ranges. The accuracy is at its worst as  $V_{VAO}$  approaches 1 V because the error of the  $(V_{VAO}-1)$  subtraction increases and begins to distort the IMO reference current to a greater degree.

### Enhanced Transient Response (VA Slew-Rate Correction)

Due to the low voltage loop bandwidth required to maintain proper PFC and ignore the slight 120-Hz ripple on the output, the response of ordinary controllers to input voltage and load transients will also be slow. However, the  $Q_{VFF}$  function effectively handles the line transient response with the exception of any minor adjustments needed within a  $Q_{VFF}$  level. Load transients on the other hand can only be handled by the voltage loop, therefore, the UCC28070 has been designed to improve its transient response by pulling up on the output of the voltage amplifier (VAO) with an additional 100  $\mu$ A of current in the event the VSENSE voltage drops below 93% of regulation (2.79 V). During a soft-start cycle, when VSENSE is ramping up from the 0.75-V PFC Enable threshold, the 100- $\mu$ A correction current source is disabled to ensure the gradual and controlled ramping of output voltage and current during a soft start.

### Voltage Biasing (VCC and VREF)

The UCC28070 operates within a VCC bias supply range of 10 V to 21 V. An Under-Voltage Lock-Out (UVLO) threshold prevents the PFC from activating until  $V_{CC} > 10.2$  V, and 1 V of hysteresis assures reliable start-up from a possibly low-compliance bias source. An internal 25-V zener-like clamp on VCC is intended only to protect the device from brief energy-limited surges from the bias supply, and should NOT be used as a regulator with a current-limited source.

At minimum, a 0.1- $\mu$ F ceramic bypass capacitor must be applied from VCC to GND close to the device pins to provide local filtering of the bias supply. Larger values may be required depending on  $I_{CC}$  peak current magnitudes and durations to minimize ripple voltage on VCC.

In order to provide a smooth transition out of UVLO and to make the 6-V voltage reference available as early as possible, the VREF output is enabled when VCC exceeds 8 V typically.

The VREF circuitry is designed to provide the biasing of all internal control circuits and for limited use externally. At minimum, a 22-nF ceramic bypass capacitor must be applied from VREF to GND close to the device pins to ensure stability of the circuit. External load current on VREF should be limited to less than 2 mA, or degraded regulation may result.

### PFC Enable and Disable

The UCC28070 contains two independent circuits dedicated to disabling the GDx outputs based on the biasing conditions of the VSENSE or SS pins. The first circuit which monitors the  $V_{VSENSE}$ , is the traditional PFC Enable that holds off soft-start and the overall PFC function until the output has pre-charged to ~25%. Prior to  $V_{VSENSE}$  reaching 0.75 V, almost all of the internal circuitry is disabled. Once  $V_{VSENSE}$  reaches 0.75 V and  $V_{AO} < 0.75$  V, the oscillator, multiplier, and current synthesizer are enabled and the SS circuitry begins to ramp up the voltage on the SS pin. The second circuit provides an external interface to emulate an internal fault condition to disable the GDx output without fully disabling the voltage loop and multiplier. By externally pulling the SS pin below 0.6 V, the GDx outputs are immediately disabled and held low. Assuming no other fault conditions are present, normal PWM operation resumes when the external SS pull-down is released. It must be noted that the external pull-down needs to be sized large enough to override the internal 1.5-mA adaptive SS pull-up once the SS voltage falls below the disable threshold. It is recommended that a MOSFET with less than 100- $\Omega$   $R_{DS(on)}$  resistance be used to ensure the SS pin is held adequately below the disable threshold.

**Adaptive Soft Start**

In order to maintain a controlled power up, the UCC28070 has been designed with an adaptive soft-start function that overrides the internal reference voltage with a controlled voltage ramp during power up. On initial power up, once  $V_{VSENSE}$  exceeds the 0.75-V enable threshold ( $V_{EN}$ ), the internal pull down on the SS pin is released, and the 1.5-mA adaptive soft-start current source is activated. This 1.5-mA pull-up almost immediately pulls the SS pin to 0.75 V ( $V_{VSENSE}$ ) to bypass the initial 25% of dead time during a traditional 0 V to  $V_{regulation}$  SS ramp. Once the SS pin has reached the voltage on  $VSENSE$ , the 10- $\mu$ A soft-start current ( $I_{SS}$ ) takes over. Thus, through the selection of the soft-start capacitor ( $C_{SS}$ ), the effective soft-start time ( $t_{SS}$ ) may be easily programmed based on the equation below.

$$t_{SS} = C_{SS} \times \left( \frac{2.25V}{10\mu A} \right) \tag{21}$$

Often, a system restart is desired following a brief shut-down. In such a case,  $VSENSE$  may still have substantial voltage if  $V_{OUT}$  has not fully discharged or if high line has peak charged  $C_{OUT}$ . To eliminate the delay caused by charging  $C_{SS}$  from 0 V up to the pre-charged  $V_{VSENSE}$  with only the 10- $\mu$ A current source and minimize any further output voltage sag, the adaptive soft start uses a 1.5-mA current source to rapidly charge  $C_{SS}$  to  $V_{VSENSE}$ , after which time the 10- $\mu$ A source controls the  $V_{SS}$  accent to the desired soft-start ramp rate. In such a case,  $t_{SS}$  is estimated as follows:

$$t_{SS} = C_{SS} \times \left( \frac{3V - V_{VSENSE0}}{10\mu A} \right) \tag{22}$$

where  $V_{VSENSE0}$  is the voltage at  $VSENSE$  at the moment a soft start or restart is initiated.

**NOTE:**

For soft start to be effective and avoid overshoot on  $V_{OUT}$ , the SS ramp must be slower than the voltage-loop control response. Choose  $C_{SS} \geq C_{VZ}$  to ensure this.

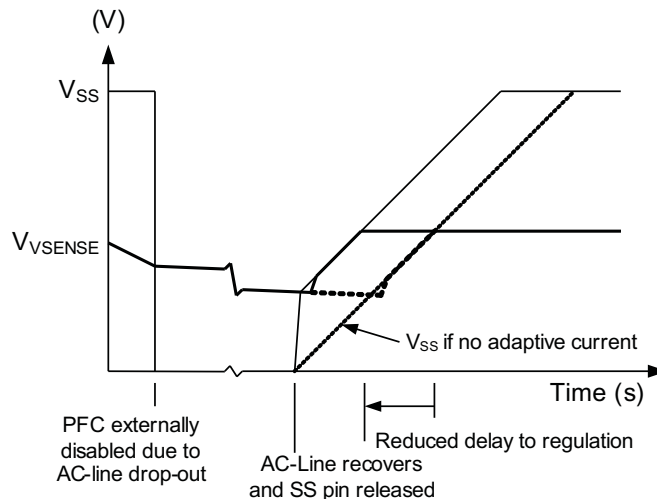


**Figure 21. Soft-Start Ramp Rate**



### **PFC Start-Up Hold Off**

An additional feature designed into the UCC28070 is the “Start-Up Hold Off” logic that prevents the device from initiating a soft-start cycle until the VAO is below the zero-power threshold (0.75 V). This feature ensures that the SS cycle will initiate from zero-power and zero duty-cycle while preventing the potential for any significant inrush currents due to stored charge in the VAO compensation network.

### **Output Over-Voltage Protection (OVP)**

Because of the high voltage output and a limited design margin on the output capacitor, output over-voltage protection is essential for PFC circuits. The UCC28070 implements OVP through the continuous monitoring of the VSENSE voltage. In the event  $V_{VSENSE}$  rises above 106% of regulation (3.18 V), the GDx outputs are immediately disabled to prevent the output voltage from reaching excessive levels. Meanwhile the CA0x outputs are pulled low in order to ensure a controlled recovery starting from 0% duty-cycle after an OVP fault is released. Once the  $V_{VSENSE}$  voltage has dropped below 3.08 V, the PWM operation resumes normal operation.

### **Zero-Power Detection**

In order to prevent undesired performance under no-load and near no-load conditions, the UCC28070 zero-power detection comparator is designed to disable both GDA and GDB output in the event the VAO voltage falls below 0.75 V. The 150 mV of hysteresis ensures that the output remains disabled until the VAO has nearly risen back into the linear range of the multiplier ( $VAO \geq 0.9$  V).

### **Thermal Shutdown**

In order to protect the power supplies from silicon failures at excessive temperatures, the UCC28070 has an internal temperature-sensing comparator that shuts down nearly all of the internal circuitry, and disables the GDA and GDB outputs, if the die temperature rises above 160°C. Once the die temperature falls below 140°C, the device brings the outputs up through a typical soft start.

**Current Loop Compensation**

The UCC28070 incorporates two identical and independent transconductance-type current-error amplifiers (one for each phase) with which to control the shaping of the PFC input current waveform. The current-error amplifier (CA) forms the heart of the embedded current control loop of the boost PFC pre-regulator, and is compensated for loop stability using familiar principles [4, 5]. The output of the CA for phase-A is CAO<sub>A</sub>, and that for phase-B is CAO<sub>B</sub>. Since the design considerations are the same for both, they are collectively referred to as CAO<sub>x</sub>, where the "x" may be "A" or "B".

In a boost PFC pre-regulator, the current control loop comprises the boost power plant stage, the current sensing circuitry, the wave-shape reference, the PWM stage, and the CA with compensation components. The CA compares the average boost inductor current sensed with the wave-shape reference from the multiplier stage and generates an output current proportional to the difference.

This CA output current flows through the impedance of the compensation network generating an output voltage, V<sub>CAO</sub>, which is then compared with a periodic voltage ramp to generate the PWM signal necessary to achieve PFC.

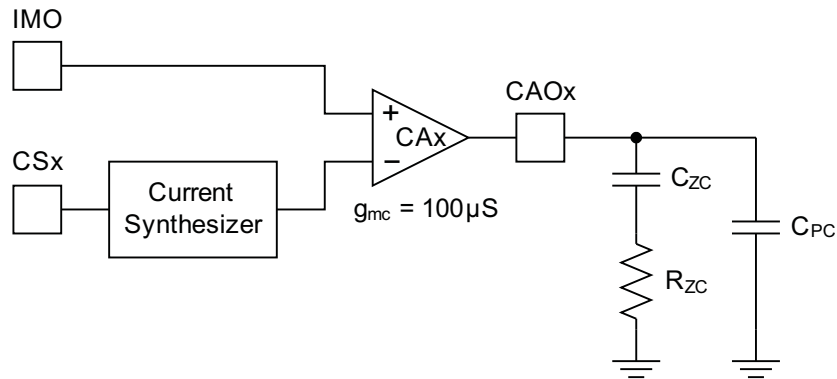


**Figure 22. Current Error Amplifier With Type II Compensation**

For frequencies above boost LC resonance and below f<sub>PWM</sub>, the small-signal model of the boost stage, which includes current sensing, can be simplified to:

$$\frac{v_{RS}}{v_{CA}} = \frac{V_{out} \times R_s / N_{CT}}{\Delta V_{RMP} \times k_{SYNC} \times s \times L_B} \tag{23}$$

where L<sub>B</sub> = mid-value boost inductance, R<sub>S</sub> = CT sense resistor, N<sub>CT</sub> = CT turns ratio, V<sub>OUT</sub> = average output voltage, ΔV<sub>RMP</sub> = 4V<sub>pk-pk</sub> amplitude of the PWM voltage ramp, k<sub>SYNC</sub> = ramp reduction factor (if PWM frequency is synchronized to an external oscillator; k<sub>SYNC</sub> = 1 otherwise), s = Laplace complex variable

An R<sub>ZC</sub>C<sub>ZC</sub> network is introduced on CAO<sub>x</sub> to obtain high gain for the low-frequency content of the inductor current signal, but reduced flat gain above the zero frequency out to f<sub>PWM</sub> to attenuate the high-frequency switching ripple content of the signal (thus averaging it).

The switching ripple voltage should be attenuated to less than 1/10 of the  $\Delta V_{RMP}$  amplitude so as to be considered “negligible” ripple.

Thus, CAOx gain at  $f_{PWM}$  is:

$$g_{mc} R_{ZC} \leq \frac{\Delta V_{RMP} \times k_{SYNC}}{\Delta I_{LB} \times \frac{R_S}{N_{CT}}} \times \frac{10}{10} \quad (24)$$

where  $\Delta I_{LB}$  is the maximum peak-to-peak ripple current in the boost inductor, and  $g_{mc}$  is the transconductance of the CA, 100  $\mu S$ .

$$R_{ZC} \leq \frac{4V \times N_{CT}}{10 \times 100 \mu S \times \Delta I_{LB} \times R_S} \quad (25)$$

The current-loop cross-over frequency is then found by equating the open loop gain to 1 and solving for  $f_{CXO}$ :

$$f_{CXO} = \frac{V_{out} \times \frac{R_S}{N_{CT}}}{\Delta V_{RMP} \times k_{SYNC} \times 2\pi \times L_B} \times g_{mc} R_{ZC} \quad (26)$$

$C_{CZ}$  is then determined by setting  $f_{ZC} = f_{CXO} = 1/(2\pi \times R_{ZC} \times C_{ZC})$  and solving for  $C_{ZC}$ . At  $f_{ZC} = f_{CXO}$ , a phase margin of 45° is obtained at  $f_{CXO}$ . Greater phase margin may be had by placing  $f_{ZC} < f_{CXO}$ .

An additional high-frequency pole is generally added at  $f_{PWM}$  to further attenuate ripple and noise at  $f_{PWM}$  and higher. This is done by adding a small-value capacitor,  $C_{pc}$ , across the  $R_{ZC} C_{ZC}$  network.

$$C_{pc} = \frac{1}{2\pi \times f_{PWM} \times R_{ZC}} \quad (27)$$

The procedure above is valid for fixed-value inductors.

**NOTE:**

If a “swinging-choke” boost inductor (inductance decreases with increasing current) is used,  $f_{CXO}$  varies with inductance, so  $C_{ZC}$  should be determined at maximum inductance.

## Voltage Loop Compensation

The outer voltage control loop of the dual-phase PFC controller functions the same as with a single-phase controller, and compensation techniques for loop stability are standard [4]. The bandwidth of the voltage-loop must be considerably lower than the twice-line ripple frequency ( $f_{2LF}$ ) on the output capacitor, to avoid distortion-causing correction to the output voltage. The output of the voltage-error amplifier (VA) is an input to the multiplier, to adjust the input current amplitude relative to the required output power. Variations on VAO within the bandwidth of the current loops will influence the wave-shape of the input current. Since the low-frequency ripple on  $C_{OUT}$  is a function of input power only, its peak-to-peak amplitude is the same at high-line as at low-line. Any response of the voltage-loop to this ripple will have a greater distorting effect on high-line current than on low-line current. Therefore, the allowable percentage of 3rd-harmonic distortion on the input current contributed by VAO should be determined using high-line conditions.

Because the voltage-error amplifier (VA) is a transconductance type of amplifier, the impedance on its input has no bearing on the amplifier gain, which is determined solely by the product of its transconductance ( $g_{mv}$ ) with its output impedance ( $Z_{OV}$ ). Thus the VSENSE input divider-network values are determined separately, based on criteria discussed in the VINAC section. Its output is the VAO pin.

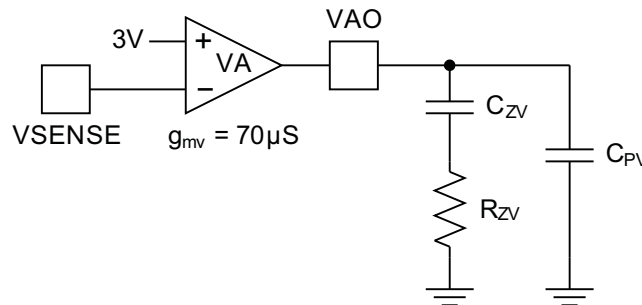


**Figure 23. Voltage Error Amplifier With Type II Compensation**

The twice-line ripple voltage component of VSENSE must be sufficiently attenuated and phase-shifted at VAO to achieve the desired level of 3rd-harmonic distortion of the input current wave-shape [4]. For every 1% of 3rd-harmonic input distortion allowable, the small-signal gain  $G_{VEA} = V_{VAOpk} / V_{SENSEpk} = g_{mv} \times Z_{OV}$  at the twice-line frequency should allow no more than 2% ripple over the full VAO voltage range. In the UCC28070,  $V_{VAO}$  can range from 1 V at zero load power to ~4.2 V (see note below) at full load power for a  $\Delta V_{VAO} = 3.2$  V, so 2% of 3.2 V is 64-mV peak ripple.

### NOTE:

Although the maximum VAO voltage is clamped at 5 V, at full load  $V_{VAO}$  may vary around an approximate center point of 4.2 V to compensate for the effects of the quantized feed-forward voltage in the multiplier stage (see Multiplier Section for details). Therefore, 4.2 V is the proper voltage to use to represent maximum output power when performing voltage-loop gain calculations.

The output capacitor maximum low-frequency zero-to-peak ripple voltage is closely approximated by:

$$V_{0pk} = \frac{Pin_{avg} \times X_{Cout}}{Vout_{avg}} = \frac{Pin_{avg}}{Vout_{avg} \times 2\pi \times f_{2LF} \times Cout} \quad (28)$$

where  $P_{IN(avg)}$  is the total maximum input power of the interleaved-PFC pre-regulator,  $V_{OUT(avg)}$  is the average output voltage and  $C_{OUT}$  is the output capacitance.

$V_{SENSEpk} = V_{opk} \times k_R$ , where  $k_R$  is the gain of the resistor-divider network on  $V_{SENSE}$ .

Thus, for  $k_{3rd}\%$  of allowable 3rd-harmonic distortion on the input current attributable to the VAO ripple,

$$Z_{OV(f_{2LF})} = \frac{k_{3rd} \times 64mV \times Vout_{avg} \times 2\pi f_{2LF} \times Cout}{g_{mv} \times k_R \times Pin_{avg}} \quad (29)$$

This impedance on VAO is set by a capacitor ( $C_{pv}$ ), where  $C_{PV} = 1/(2\pi f_{2LF} \times Z_{OV}(f_{2LF}))$  therefore,

$$C_{pv} = \frac{g_{mv} \times k_R \times Pin_{avg}}{k_{3rd} \times 64mV \times Vout_{avg} \times (2\pi f_{2LF})^2 \times Cout} \quad (30)$$

The voltage-loop unity-gain cross-over frequency ( $f_{VXO}$ ) may now be solved by setting the open-loop gain equal to 1:

$$TV(f_{VXO}) = G_{BST} \times G_{VEA} \times k_R = \left( \frac{Pin_{avg} \times X_{Cout}}{\Delta V_{VAO} \times Vout_{avg}} \right) \times (g_{mv} \times X_{Cpv}) \times k_R = 1 \quad (31)$$

so,

$$f_{VXO}^2 = \frac{g_{mv} \times k_R \times Pin_{avg}}{\Delta V_{VAO} \times Vout_{avg} \times (2\pi)^2 \times Cpv \times Cout} \quad (32)$$

The “zero-resistor” ( $R_{ZV}$ ) from the zero-placement network of the compensation may now be calculated. Together with  $C_{PV}$ ,  $R_{ZV}$  sets a pole right at  $f_{VXO}$  to obtain 45° phase margin at the cross-over.

Thus,

$$R_{ZV} = \frac{1}{2\pi f_{VXO} \times Cpv} \quad (33)$$

Finally, a zero is placed at or below  $f_{VXO}/6$  with capacitor  $C_{ZV}$  to provide high gain at dc but with a breakpoint far enough below  $f_{VXO}$  so as not to significantly reduce the phase margin. Choosing  $f_{VXO}/10$  allows one to approximate the parallel combination value of  $C_{ZV}$  and  $C_{PV}$  as  $C_{ZV}$ , and solve for  $C_{ZV}$  simply as:

$$C_{ZV} = \frac{10}{2\pi f_{VXO} \times R_{ZV}} \approx 10 \times Cpv \quad (34)$$

By using a spreadsheet or math program,  $C_{ZV}$ ,  $R_{ZV}$ , and  $C_{PV}$  may be manipulated to observe their effects on  $f_{VXO}$  and phase margin and %-contribution to 3rd-harmonic distortion (see note below). Also, phase margin may be checked as  $P_{IN(avg)}$  level and system parameter tolerances vary.

**NOTE:**

The percent of 3rd-harmonic distortion calculated in this section represents the contribution from the  $f_{2LF}$  voltage ripple on  $C_{OUT}$  only. Other sources of distortion, such as the current-sense transformer, the current synthesizer stage, even distorted  $V_{IN}$ , etc., can contribute additional 3rd and higher harmonic distortion.

## Advanced Design Techniques

### Current Loop Feedback Configuration (Sizing of the Current Transformer Turns Ratio and Sense Resistor ( $R_S$ ))

A current-sense transformer (CT) is typically used in high-power applications to sense inductor current while avoiding significant losses in the sensing resistor. For average current-mode control, the entire inductor current waveform is required; however low-frequency CTs are obviously impracticable. Normally, two high-frequency CTs are used, one in the switching leg to obtain the up-slope current and one in the diode leg to obtain the down-slope current. These two current signals are summed together to form the entire inductor current, but this is not the case for the UCC28070.

A major advantage of the UCC28070 design is the current synthesis function, which internally recreates the inductor current down-slope during the switching period off-time. This eliminates the need for the diode-leg CT in each phase, significantly reducing space, cost and complexity. A single resistor programs the synthesizer down slope, as previously discussed in the Current Synthesizer section.

A number of trade-offs must be made in the selection of the CT. Various internal and external factors influence the size, cost, performance, and distortion contribution of the CT.

These factors include, but are not limited to:

- Turns-ratio ( $N_{CT}$ )
- Magnetizing inductance ( $L_M$ )
- Leakage inductance ( $L_{LK}$ )
- Volt-microsecond product ( $V_{\mu s}$ )
- Distributed capacitance ( $C_d$ )
- Series resistance ( $R_{SER}$ )
- External diode drop ( $V_D$ )
- External current sense resistor ( $R_S$ )
- External reset network

Traditionally, the turns-ratio and the current sense resistor are selected first. Some iterations may be needed to refine the selection once the other considerations are included.

In general,  $50 \leq N_{CT} \leq 200$  is a reasonable range from which to choose. If  $N_{CT}$  is too low, there may be high power loss in  $R_S$  and insufficient  $L_M$ . If too high, there could be excessive  $L_{LK}$  and  $C_d$ . (A one-turn primary winding is assumed.)

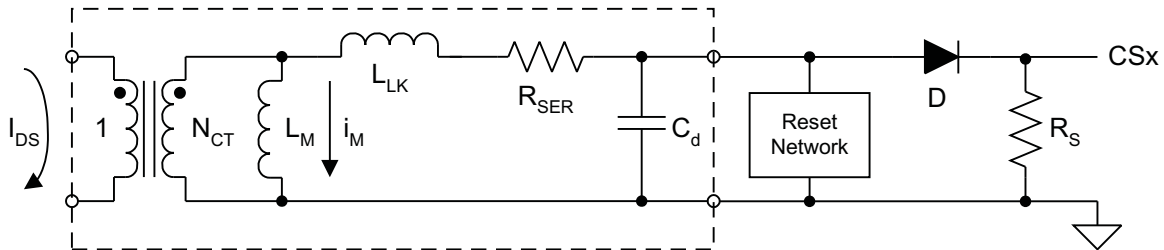


**Figure 24. Current Sense Transformer Equivalent Circuit**

A major contributor to distortion of the input current is the effect of magnetizing current on the CT output signal ( $i_{RS}$ ). A higher turns-ratio results in a higher  $L_M$  for a given core size.  $L_M$  should be high enough that the magnetizing current ( $i_M$ ) generated is a very small percentage of the total transformed current. This is an impossible criterion to maintain over the entire current range, because  $i_M$  unavoidably becomes a larger fraction of  $i_{RS}$  as the input current decreases toward zero. The effect of  $i_M$  is to “steal” some of the signal current away from  $R_S$ , reducing the CSx voltage and effectively understating the actual current being sensed. At low currents, this understatement can be significant and CAOx increases the current-loop duty-cycle in an attempt to correct the CSx input(s) to match the IMO reference voltage. This unwanted correction results in overstated current on the input wave shape in the regions where the CT understatement is significant, such as near the ac line zero crossings. It can affect the entire waveform to some degree under the high line, light-load conditions.

The sense resistor  $R_S$  is chosen, in conjunction with  $N_{CT}$ , to establish the sense voltage at CSx to be about 3 V at the center of the reflected inductor ripple current under maximum load. The goal is to maximize the average signal within the common-mode input range  $V_{CMCAO}$  of the CAOx current-error amplifiers, while leaving room for the peaks of the ripple current within  $V_{CMCAO}$ . The design condition should be at the lowest maximum input power limit as determined in the Multiplier Section. If the inductor ripple current is so high as to cause  $V_{CSx}$  to exceed  $V_{CMCAO}$ , then  $R_S$  or  $N_{CT}$  or both must be adjusted to reduce peak  $V_{CSx}$ , which could reduce the average sense voltage center below 3 V. There is nothing wrong with this situation; but be aware that the signal is more compressed between full- and no-load, with potentially more distortion at light loads.

The matter of volt-second balancing is important, especially with the widely varying duty-cycles in the PFC stage. Ideally, the CT is reset once each switching period; that is, the off-time  $V_{\mu s}$  product equals the on-time  $V_{\mu s}$  product. (Because a switching period is usually measured in microseconds, it is convenient to convert the volt-second product to volt-microseconds to avoid sub-decimal numbers.) On-time  $V_{\mu s}$  is the time-integral of the voltage across  $L_M$  generated by the series elements  $R_{SER}$ ,  $L_{LK}$ , D, and  $R_S$ . Off-time  $V_{\mu s}$  is the time-integral of the voltage across the reset network during the off-time. With passive reset,  $V_{\mu s-off}$  is unlikely to exceed  $V_{\mu s-on}$ . Sustained unbalance in the on or off  $V_{\mu s}$  products will lead to core saturation and a total loss of the current-sense signal. Loss of  $V_{CSx}$  causes  $V_{CAOX}$  to quickly rise to its maximum, programming a maximum duty-cycle at any line condition. This, in turn causes the boost inductor current to increase without control, until the system fuse or some component failure interrupts the input current.

It is vital that the CT has plenty of  $V_{\mu s}$  design-margin to accommodate various special situations where there to be several consecutive maximum duty-cycle periods at maximum input current, such as during peak current limiting.

Maximum  $V_{\mu s(on)}$  can be estimated by:

$$V_{\mu(on)max} = t_{ON(max)} \times (V_{RS} + V_D + V_{RSEr} + V_{LK}) \quad (35)$$

where all factors are maximized to account for worst-case transient conditions and  $t_{ON(max)}$  occurs during the lowest dither frequency when frequency dithering is enabled. For design margin, a CT rating of  $\sim 5 \cdot V_{\mu s(on)max}$  or higher is suggested. The contribution of  $V_{RS}$  varies directly with the line current. However,  $V_D$  may have a significant voltage even at near-zero current, so substantial  $V_{\mu s(on)}$  may accrue at the zero-crossings where the duty-cycle is maximum.  $V_{RSEr}$  is the least contributor, and often can be neglected if  $R_{SEr} \ll R_S$ .  $V_{LK}$  is developed by the  $di/dt$  of the sensed current, and is not observable externally. However, its impact is considerable, given the sub-microsecond rise-time of the current signal plus the slope of the inductor current. Fortunately, most of the built-up  $V_{\mu s}$  across  $L_M$  during the on-time is removed during the fall-time at the end of the duty-cycle, leaving a lower net  $V_{\mu s(on)}$  to be reset during the off-time. Nevertheless, the CT must, at the very minimum, be capable of sustaining the full internal  $V_{\mu s(on)max}$  built up until the moment of turn-off within a switching period.

$V_{\mu s(off)}$  may be generated with a resistor or zener diode, using the  $i_M$  as bias current.

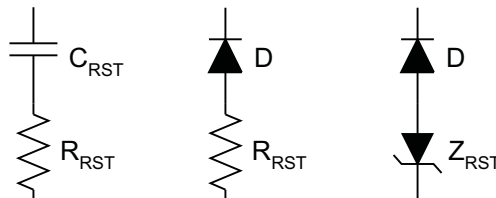


**Figure 25. Possible Reset Networks**

In order to accommodate various CT circuit designs and prevent the potentially destructive result due to CT saturation, the UCC28070's maximum duty-cycle needs to be programmed such that the resulting minimum off-time accomplishes the required worst-case reset. (See the PWM Frequency and Duty-Cycle Clamp section of the data sheet for more information on sizing  $R_{DMX}$ ) Be aware that excessive  $C_d$  in the CT can interfere with effective resetting, because the maximum reset voltage is not reached until after 1/4-period of the CT self-resonant frequency. A higher turns-ratio results in higher  $C_d$  [3], so a trade-off between  $N_{CT}$  and  $D_{MAX}$  must be made.

The selected turns-ratio also affects  $L_M$  and  $L_{LK}$ , which vary proportionally to the square of the turns. Higher  $L_M$  is good, while higher  $L_{LK}$  is not. If the voltage across  $L_M$  during the on-time is assumed to be constant (which it is not, but close enough to simplify) then the magnetizing current is an increasing ramp.

This upward ramping current subtracts from  $i_{RS}$ , which affects  $V_{CSx}$  especially heavily at the zero-crossings and light loads, as stated earlier. With a reduced peak at  $V_{CSx}$ , the current synthesizer starts the down-slope at a lower voltage, further reducing the average signal to  $CAOx$  and further increasing the distortion under these conditions. If low input current distortion at very light loads is required, special mitigation methods may need to be developed to accomplish that goal.



**Current Sense Offset and PWM Ramp for Improved Noise Immunity**

To improve noise immunity at extremely light loads, a PWM ramp with a dc offset is recommended to be added to the current sense signals. Electrical components  $R_{TA}$ ,  $R_{TB}$ ,  $R_{OA}$ ,  $R_{OB}$ ,  $C_{TA}$ ,  $C_{TB}$ ,  $D_{PA1}$ ,  $D_{PA2}$ ,  $D_{PB1}$ ,  $D_{PB2}$ ,  $C_{TA}$ ,  $C_{TB}$  form a PWM ramp that is activated and deactivated by the gate drive outputs of the UCC28070. Resistor  $R_{OA}$  and  $R_{OB}$  add a dc offset to the CS resistors ( $R_{SA}$  and  $R_{SB}$ ).

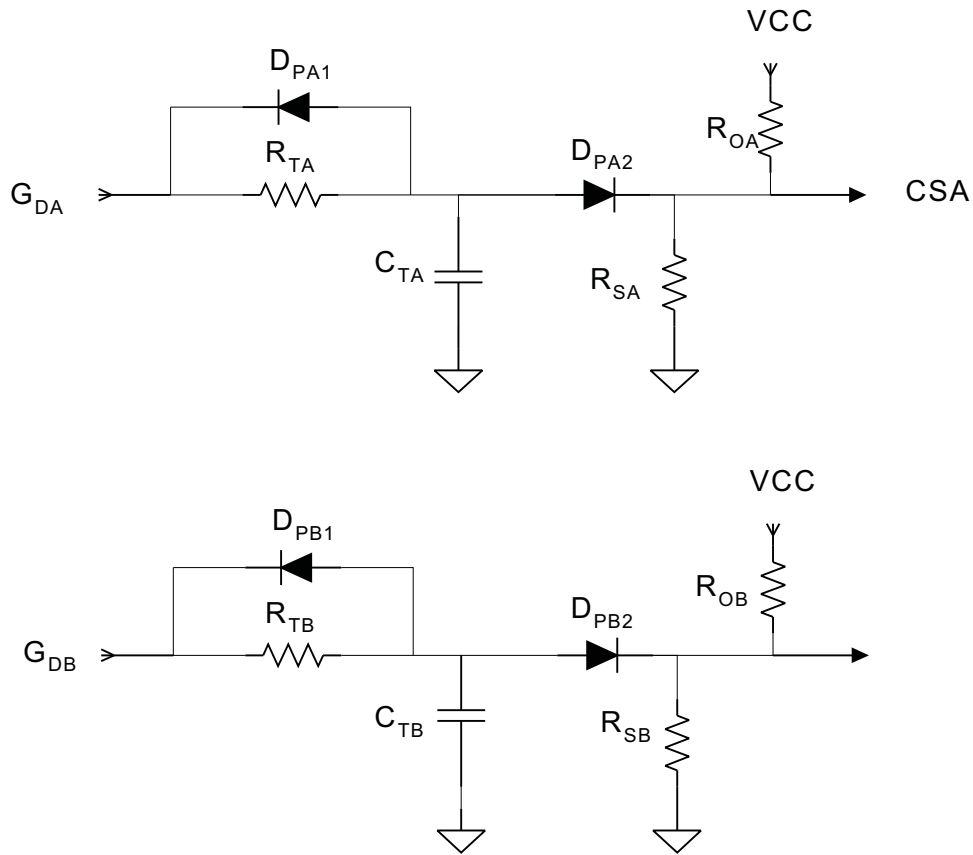


**Figure 26. PWM Ramp and Offset Circuit**

When the inductor current becomes discontinuous the boost inductors ring with the parasitic capacitances in the boost stages. This inductor current rings through the CTs causing a false current sense signal. Please refer to the following graphical representation of what the current sense signal looks like when the inductor current goes discontinuous.

**NOTE:**

The inductor current and RS may vary from this graphical representation depending on how much inductor ringing is in the design when the unit goes discontinuous.

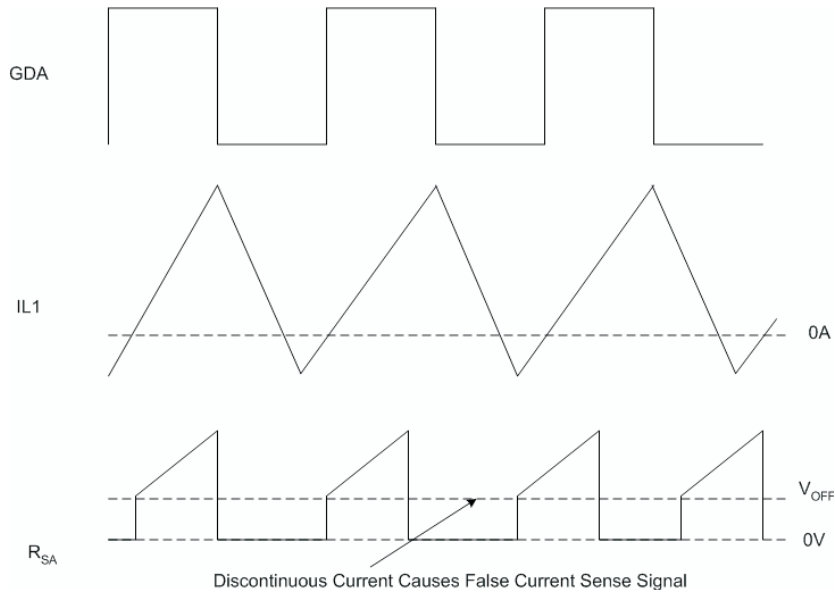


**Figure 27. False Current Sense Signal**

To counter for the offset ( $V_{OFF}$ ) just requires adjusting resistors  $R_{OA}$  and  $R_{OB}$  to ensure that when the unit goes discontinuous the current sense resistor is not seeing a positive current when it should be zero. Setting the offset to 120 mV is a good starting point and may need to be adjusted based on individual design criteria.

$$R_{SA} = R_{SB} \tag{36}$$

$$R_{OA} = R_{OB} = \frac{(V_{VCC} - V_{OFF})R_{SA}}{V_{OFF}} \tag{37}$$

A small PWM ramp that is equal to 10% of the maximum current sense signal ( $V_S$ ) less the offset can then be added by properly selecting  $R_{TA}$ ,  $R_{TB}$ ,  $C_{TA}$  and  $C_{TB}$ .

$$R_{TA} = R_{TB} = \frac{(V_{VCC} - (V_S \times 0.1 - V_{OFF}) + V_{DA2})R_{SA}}{V_S \times 0.1 - V_{OFF}} \tag{38}$$

$$C_{TA} = C_{TB} = \frac{1}{R_{TA} \times f_S \times 3} \tag{39}$$

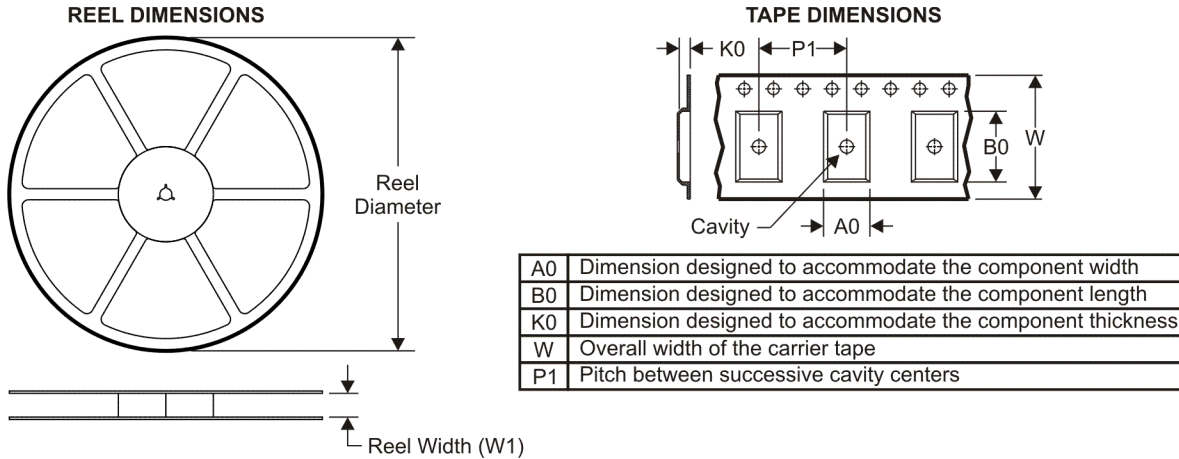
### Recommended PCB Device Layout

Interleaved PFC techniques dramatically reduce input and output ripple current caused by the PFC boost inductor, which allows the circuit to use smaller and less expensive filters. To maximize the benefits of interleaving, the output filter capacitor should be located after the two phases allowing the current of each phase to be combined together before entering the boost capacitor. Similar to other power management devices, when laying out the PCB it is important to use star grounding techniques and to keep filter and high frequency bypass capacitors as close to device pins and ground as possible. To minimize the possibility of interference caused by magnetic coupling from the boost inductor, the device should be located at least 1 inch away from the boost inductor. It is also recommended that the device not be placed underneath magnetic elements.

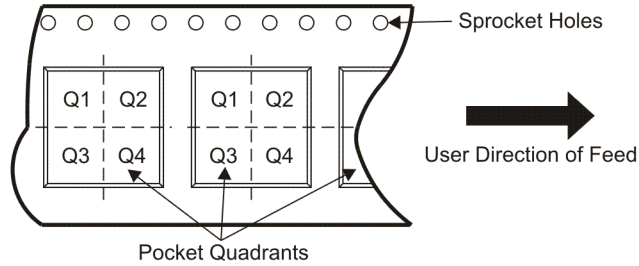
### References

1. O'Loughlin, Michael, "An Interleaving PFC Pre-Regulator for High-Power Converters", Texas Instruments, Inc. 2006 Unitrode Power Supply Seminar, Topic 5
2. Erickson, Robert W., "Fundamentals of Power Electronics", 1st ed., pp. 604-608 Norwell, MA: Kluwer Academic Publishers, 1997
3. Creel, Kirby "Measuring Transformer Distributed Capacitance", White Paper, Datatronic Distribution, Inc. website: [http://www.datatronics.com/pdf/distributed\\_capacitance\\_paper.pdf](http://www.datatronics.com/pdf/distributed_capacitance_paper.pdf)
4. L. H. Dixon, "Optimizing the Design of a High Power Factor Switching Preregulator", Unitrode Power Supply Design Seminar Manual SEM700, 1990. Texas Instruments Literature Number SLUP093
5. L. H. Dixon, "High Power Factor Preregulator for Off-Line Power Supplies", Unitrode Power Supply Design Seminar Manual SEM600, 1988. Texas Instruments Literature Number SLUP087

**TAPE AND REEL INFORMATION**



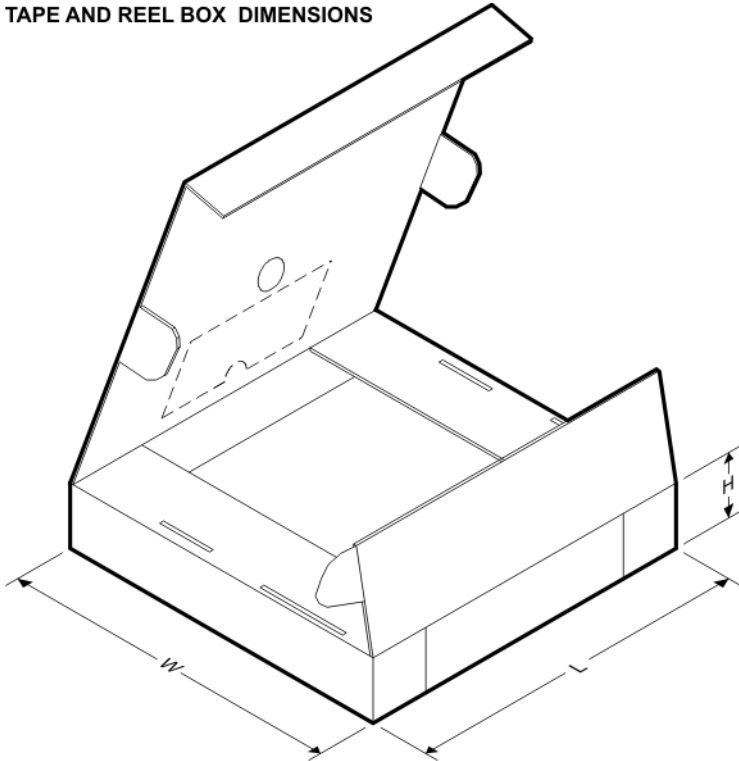
**QUADRANT ASSIGNMENTS FOR PIN 1 ORIENTATION IN TAPE**



\*All dimensions are nominal

| Device      | Package Type | Package Drawing | Pins | SPQ  | Reel Diameter (mm) | Reel Width W1 (mm) | A0 (mm) | B0 (mm) | K0 (mm) | P1 (mm) | W (mm) | Pin1 Quadrant |
|-------------|--------------|-----------------|------|------|--------------------|--------------------|---------|---------|---------|---------|--------|---------------|
| UCC28070PWR | TSSOP        | PW              | 20   | 2000 | 330.0              | 16.4               | 6.95    | 7.1     | 1.6     | 8.0     | 16.0   | Q1            |

**TAPE AND REEL BOX DIMENSIONS**



\*All dimensions are nominal

| Device      | Package Type | Package Drawing | Pins | SPQ  | Length (mm) | Width (mm) | Height (mm) |
|-------------|--------------|-----------------|------|------|-------------|------------|-------------|
| UCC28070PWR | TSSOP        | PW              | 20   | 2000 | 346.0       | 346.0      | 33.0        |

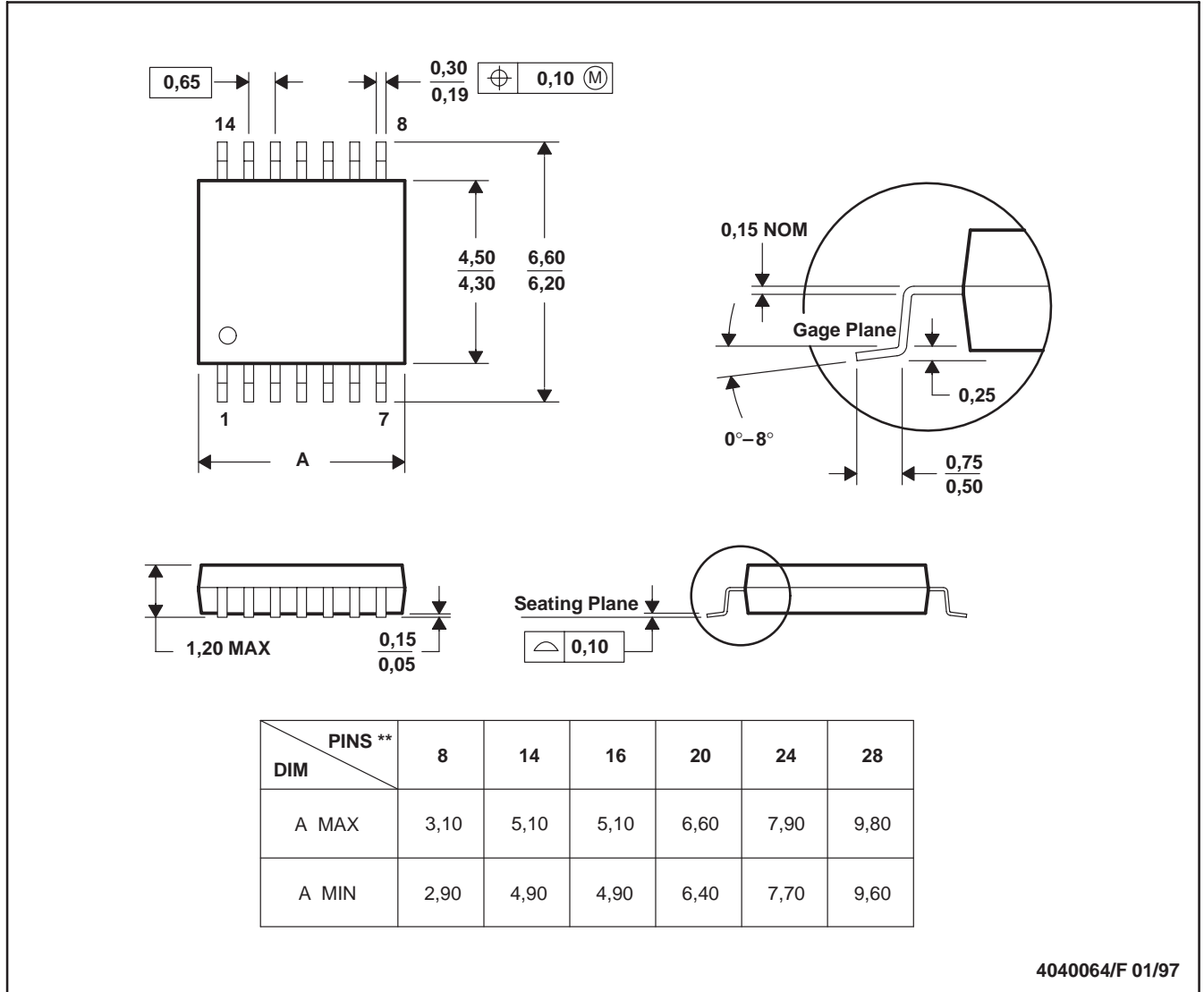
# MECHANICAL DATA

MTSS001C – JANUARY 1995 – REVISED FEBRUARY 1999

**PW (R-PDSO-G\*\*)**

**PLASTIC SMALL-OUTLINE PACKAGE**

14 PINS SHOWN



- NOTES:
- All linear dimensions are in millimeters.
  - This drawing is subject to change without notice.
  - Body dimensions do not include mold flash or protrusion not to exceed 0,15.
  - Falls within JEDEC MO-153

## IMPORTANT NOTICE

Texas Instruments Incorporated and its subsidiaries (TI) reserve the right to make corrections, modifications, enhancements, improvements, and other changes to its products and services at any time and to discontinue any product or service without notice. Customers should obtain the latest relevant information before placing orders and should verify that such information is current and complete. All products are sold subject to TI's terms and conditions of sale supplied at the time of order acknowledgment.

TI warrants performance of its hardware products to the specifications applicable at the time of sale in accordance with TI's standard warranty. Testing and other quality control techniques are used to the extent TI deems necessary to support this warranty. Except where mandated by government requirements, testing of all parameters of each product is not necessarily performed.

TI assumes no liability for applications assistance or customer product design. Customers are responsible for their products and applications using TI components. To minimize the risks associated with customer products and applications, customers should provide adequate design and operating safeguards.

TI does not warrant or represent that any license, either express or implied, is granted under any TI patent right, copyright, mask work right, or other TI intellectual property right relating to any combination, machine, or process in which TI products or services are used. Information published by TI regarding third-party products or services does not constitute a license from TI to use such products or services or a warranty or endorsement thereof. Use of such information may require a license from a third party under the patents or other intellectual property of the third party, or a license from TI under the patents or other intellectual property of TI.

Reproduction of TI information in TI data books or data sheets is permissible only if reproduction is without alteration and is accompanied by all associated warranties, conditions, limitations, and notices. Reproduction of this information with alteration is an unfair and deceptive business practice. TI is not responsible or liable for such altered documentation. Information of third parties may be subject to additional restrictions.

Resale of TI products or services with statements different from or beyond the parameters stated by TI for that product or service voids all express and any implied warranties for the associated TI product or service and is an unfair and deceptive business practice. TI is not responsible or liable for any such statements.

TI products are not authorized for use in safety-critical applications (such as life support) where a failure of the TI product would reasonably be expected to cause severe personal injury or death, unless officers of the parties have executed an agreement specifically governing such use. Buyers represent that they have all necessary expertise in the safety and regulatory ramifications of their applications, and acknowledge and agree that they are solely responsible for all legal, regulatory and safety-related requirements concerning their products and any use of TI products in such safety-critical applications, notwithstanding any applications-related information or support that may be provided by TI. Further, Buyers must fully indemnify TI and its representatives against any damages arising out of the use of TI products in such safety-critical applications.

TI products are neither designed nor intended for use in military/aerospace applications or environments unless the TI products are specifically designated by TI as military-grade or "enhanced plastic." Only products designated by TI as military-grade meet military specifications. Buyers acknowledge and agree that any such use of TI products which TI has not designated as military-grade is solely at the Buyer's risk, and that they are solely responsible for compliance with all legal and regulatory requirements in connection with such use.

TI products are neither designed nor intended for use in automotive applications or environments unless the specific TI products are designated by TI as compliant with ISO/TS 16949 requirements. Buyers acknowledge and agree that, if they use any non-designated products in automotive applications, TI will not be responsible for any failure to meet such requirements.

Following are URLs where you can obtain information on other Texas Instruments products and application solutions:

| <b>Products</b>             |  | <b>Applications</b> |  |
|-----------------------------|--|---------------------|--|
| Amplifiers                  | <a href="http://amplifier.ti.com">amplifier.ti.com</a>             | Audio               | <a href="http://www.ti.com/audio">www.ti.com/audio</a>                   |
| Data Converters             | <a href="http://dataconverter.ti.com">dataconverter.ti.com</a>     | Automotive          | <a href="http://www.ti.com/automotive">www.ti.com/automotive</a>         |
| DSP                         | <a href="http://dsp.ti.com">dsp.ti.com</a>                         | Broadband           | <a href="http://www.ti.com/broadband">www.ti.com/broadband</a>           |
| Clocks and Timers           | <a href="http://www.ti.com/clocks">www.ti.com/clocks</a>           | Digital Control     | <a href="http://www.ti.com/digitalcontrol">www.ti.com/digitalcontrol</a> |
| Interface                   | <a href="http://interface.ti.com">interface.ti.com</a>             | Medical             | <a href="http://www.ti.com/medical">www.ti.com/medical</a>               |
| Logic                       | <a href="http://logic.ti.com">logic.ti.com</a>                     | Military            | <a href="http://www.ti.com/military">www.ti.com/military</a>             |
| Power Mgmt                  | <a href="http://power.ti.com">power.ti.com</a>                     | Optical Networking  | <a href="http://www.ti.com/opticalnetwork">www.ti.com/opticalnetwork</a> |
| Microcontrollers            | <a href="http://microcontroller.ti.com">microcontroller.ti.com</a> | Security            | <a href="http://www.ti.com/security">www.ti.com/security</a>             |
| RFID                        | <a href="http://www.ti-rfid.com">www.ti-rfid.com</a>               | Telephony           | <a href="http://www.ti.com/telephony">www.ti.com/telephony</a>           |
| RF/IF and ZigBee® Solutions | <a href="http://www.ti.com/lprf">www.ti.com/lprf</a>               | Video & Imaging     | <a href="http://www.ti.com/video">www.ti.com/video</a>                   |
|                             |  | Wireless            | <a href="http://www.ti.com/wireless">www.ti.com/wireless</a>             |

Mailing Address: Texas Instruments, Post Office Box 655303, Dallas, Texas 75265  
Copyright © 2008, Texas Instruments Incorporated